

Research Paper

Compressional origin of the Aegean Orogeny, Greece

Michael P. Searle^{a,*}, Thomas N. Lamont^{a,b}^a Dept. Earth Sciences, Oxford University, South Parks Road, Oxford, OX1 3AN, UK^b School of Earth and Environmental Sciences, University of St Andrews, St Andrews, KY169AL, UK

ARTICLE INFO

Keywords:

Cyclades

Ophiolite

High-pressure metamorphism

Core complex

Compressional tectonics

ABSTRACT

The Aegean Sea area is thought to be an actively extending back-arc region, north of the present day Hellenic volcanic arc and north-dipping subduction zone in the Eastern Mediterranean. The area shows extensive normal faulting, ductile 'extensional' shear zones and extensional S-C fabrics throughout the islands that have previously been related to regional Aegean extension associated with slab rollback on the Hellenic Subduction Zone. In this paper, we question this interpretation, and suggest the Cenozoic geodynamic evolution of the Aegean region is associated with a Late Cretaceous–Eocene NE-dipping subduction zone that was responsible for continent-continent collision between Eurasia and Adria-Apulia/Cyclades. Exhumation of eclogite and blueschist facies rocks in the Cyclades and kyanite-sillimanite grade gneisses in the Naxos core complex have pressures that are far greater than could be accounted for purely by lithospheric extension and isostatic uplift. We identify four stages of crustal shortening that affected the region prior to regional lithospheric extension, herein called the Aegean Orogeny. This orogeny followed a classic Wilson cycle from early ophiolite obduction (ca. 74 Ma) onto a previously passive continental margin, to attempted crustal subduction with HP eclogite and blueschist facies metamorphism (ca. 54–45 Ma), through crustal thickening and regional kyanite – sillimanite grade Barrovian-type metamorphism (ca. 22–14 Ma), to orogenic collapse (<14 Ma). At least three periods of 'extensional' fabrics relate to: (1) Exhumation of blueschists and eclogite facies rocks showing tight-isoclinal folds and top-NE, base-SW fabrics, recording return flow along a subduction channel in a compressional tectonic setting (ca. 50–35 Ma). (2) Extensional fabrics within the core complexes formed by exhumation of kyanite- and sillimanite gneisses showing thrust-related fabrics at the base and 'extensional' fabrics along the top (ca. 18.5–14 Ma). (3) Regional ductile-brittle 'extensional' fabrics and low-angle normal faulting related to the North Cycladic Detachment (NCD) and the South(West) Cycladic Detachment (WCD) during regional extension along the flanks of a major NW–SE anticlinal fold along the middle of the Cyclades. Major low-angle normal faults and ductile shear zones show symmetry about the area, with the NE chain of islands (Andros, Tinos, Mykonos, Icaria) exposing the NE-dipping NCD with consistent top-NE ductile fabrics along 200 km of strike. In contrast, from the Greek mainland (Attica) along the SE chain of islands (Kea, Kythnos, Serifos) a SW-dipping low-angle normal fault and ductile shear zone, the WCD is inferred for at least 100 km along strike. Islands in the middle of the Cyclades show deeper structural levels including kyanite- and sillimanite-grade metamorphic core complexes (Naxos, Paros) as well as Variscan basement rocks (Naxos, Ios). The overall structure is an ~100 km wavelength NW–SE trending dome with low-angle extensional faults along each flank, dipping away from the anticline axis to the NE and SW. Many individual islands show post-extensional large-scale folding of the low-angle normal faults around the domes (Naxos, Paros, Ios, Sifnos) indicating a post-Miocene late phase of E–W shortening.

1. Introduction

The Aegean Sea region in southern Greece is regarded as a type example of an actively extending piece of continental crust and lithosphere associated with orogenic collapse of previously thickened crust

(Fig. 1; e.g. Lister et al., 1984; Jolivet, 2001; Jolivet et al., 2009a, 2009b, 2010; Jolivet and Brun, 2010; Menant et al., 2016). GPS data shows a SW 'flowing' extension direction, away from the thick crust in Anatolia (McClusky et al., 2000; Reilinger et al., 2006; Dilek and Sandvol, 2009), and earthquakes record E–W extension across the region (Kokkalas and

* Corresponding author.

E-mail address: Mike.Searle@earth.ox.ac.uk (M.P. Searle).

Peer-review under responsibility of China University of Geosciences (Beijing).

<https://doi.org/10.1016/j.gsf.2020.07.008>

Received 3 March 2020; Received in revised form 5 July 2020; Accepted 15 July 2020

Available online 7 August 2020

1674-9871/© 2020 China University of Geosciences (Beijing) and Peking University. Production and hosting by Elsevier B.V. This is an open access article under the

CC BY-NC-ND license (<http://creativecommons.org/licenses/by-nc-nd/4.0/>).

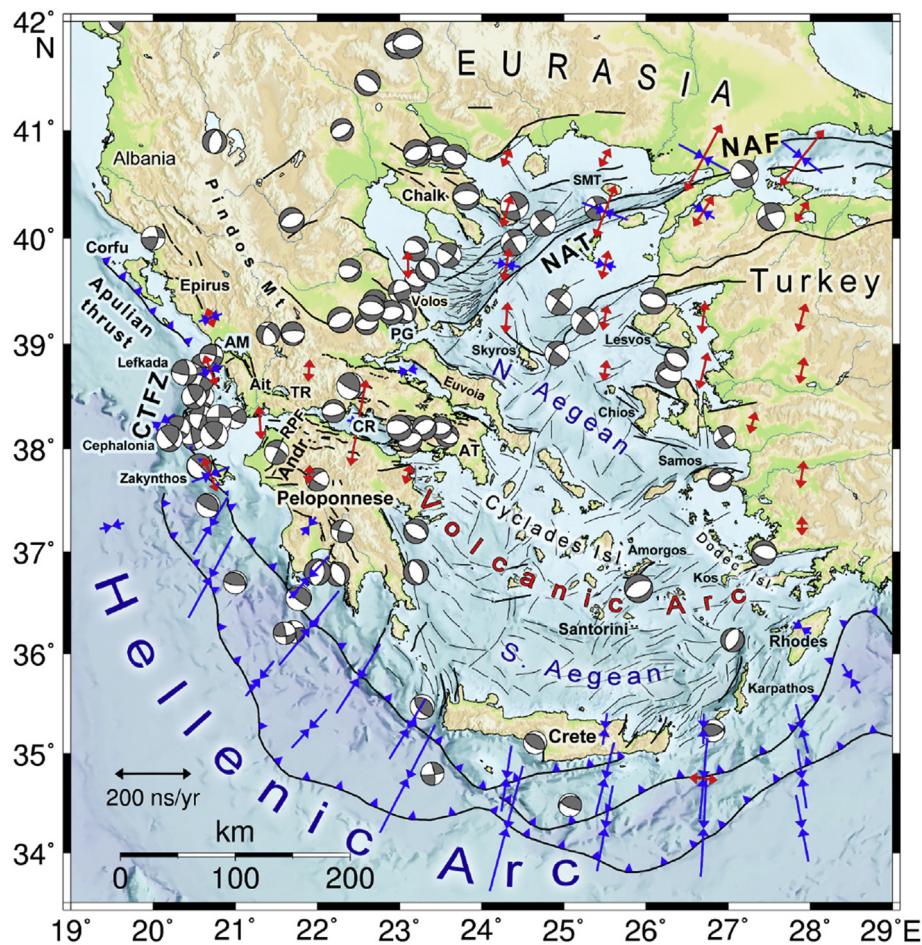


Fig. 1. Regional map of the Eastern Mediterranean region, after Kapetanidis and Kassaras (2019). Blue arrows show directions of maximum shortening; red arrows show direction of extension; selected focal mechanisms of earthquakes ($M_w > 6.0$) are shown. NAT – North Aegean Trough; NAF – Anatolian Fault; CR – Corinth rift; CTFZ – Cephalonia Transform Fault zone; RPF – Rion-Patras Fault zone; AT – Attica; PG – Pagasetikos Gulf; AM – Ambracian Gulf; SMT – Samotrace; TR – Trikala.

Doutsos, 2001; Shaw and Jackson, 2010; Kapetanidis and Kassaras, 2019). The geology of the Cyclades islands has been extensively studied by numerous authors, many of whom are referenced in the appropriate sections that follow. Fig. 2 is a geological map of the Cyclades islands and Fig. 3 shows two cross-sections showing the simplified structure. This paper is a regional review of the geology of the Cyclades Islands in the reference frame of the complete orogenic cycle. It is meant to pull together evidence for each stage of the orogenic cycle, different parts of which are exposed on individual islands, and to draw comparisons with other well-known orogenic belts such as Oman and the Himalaya. Fig. 4 shows a comparative tectonic stratigraphy for several key islands, showing the major geological units and major shear zones, detachments and low-angle normal faults.

The geology of the Cyclades Islands shows six major geological units that can be summarised as: (a) obducted ophiolite complexes (e.g. Tsiknias Ophiolite on Tinos island); (b) extensive eclogites and blueschists (Cycladic Blueschist Unit) with an amphibolite - greenschist facies overprint, related to NE-directed subduction of oceanic crust and continental margin rocks, and SW-directed exhumation (e.g. Zas Unit on Naxos); (c) proximal continental margin sedimentary rocks deposited along the previously NE passive margin of the Adria-Apulia plate, subsequently buried to HP and kyanite-grade metamorphic depths (e.g. Koronos unit on Naxos); (d) core Unit of the Naxos core complex comprising sillimanite grade migmatites and gneisses; (e) Adria-Apulia plate Variscan basement rocks (Ios), and (f) late orogenic I and S-type granite intrusions ranging of ~15–8 Ma.

All of these rocks are truncated by the major low-angle normal faults

that cut across the highest and intermediate structural levels (e.g. North Cycladic Detachment [NCD] on Mykonos, Tinos and Andros, Naxos-Paros Detachment [NPD] on Naxos and Paros, West Cycladic Detachment [WCD] on Attica, Kea and Serifos, and the Santorini Detachment [SD] on Santorini). Several previous studies have mostly related extensional fabrics in all units to regional Aegean lithospheric extension in the back-arc region (Lister et al., 1984; Jolivet et al., 2009a, 2009b; Jolivet and Brun, 2010; Whitney et al., 2013). However, several authors have proposed a compressional channel flow origin for exhumation of the Cycladic blueschists (e.g. Chatzaras et al., 2006; Xypolias et al., 2003; Xypolias and Kokkalas, 2006; Xypolias et al., 2012; Ring et al., 2007, 2011, 2020; Huet et al., 2009; Xypolias and Alsop, 2014; Aravadinou and Xypolias, 2017). Recently, Lamont et al. (2019) and Searle and Lamont (2019) proposed that the Naxos core complex, both the inner core (sillimanite grade migmatites) and outer core (kyanite grade gneisses; e.g. Koronos Unit) were formed in a compressional environment prior to large-scale Aegean extension. Structural mapping combined with extensive U–Pb zircon and monazite dating of all units on Naxos has confirmed that extensional fabrics along the NPD truncate compressional upright folds in the core and recumbently folded nappes in the Koronos Unit (Lamont et al., 2019). Extensional fabrics in all tectonic units have frequently been misinterpreted and assigned to regional Aegean lithospheric extension. We propose that many of these structures and fabrics are related to exhumation of the HP subduction channel (following Chatzaras et al., 2006; Xypolias et al., 2003; Xypolias and Kokkalas, 2006; Xypolias et al., 2012; Ring et al., 2007, 2011, 2020; Huet et al., 2009; Xypolias and Alsop, 2014; Aravadinou and Xypolias, 2017), or

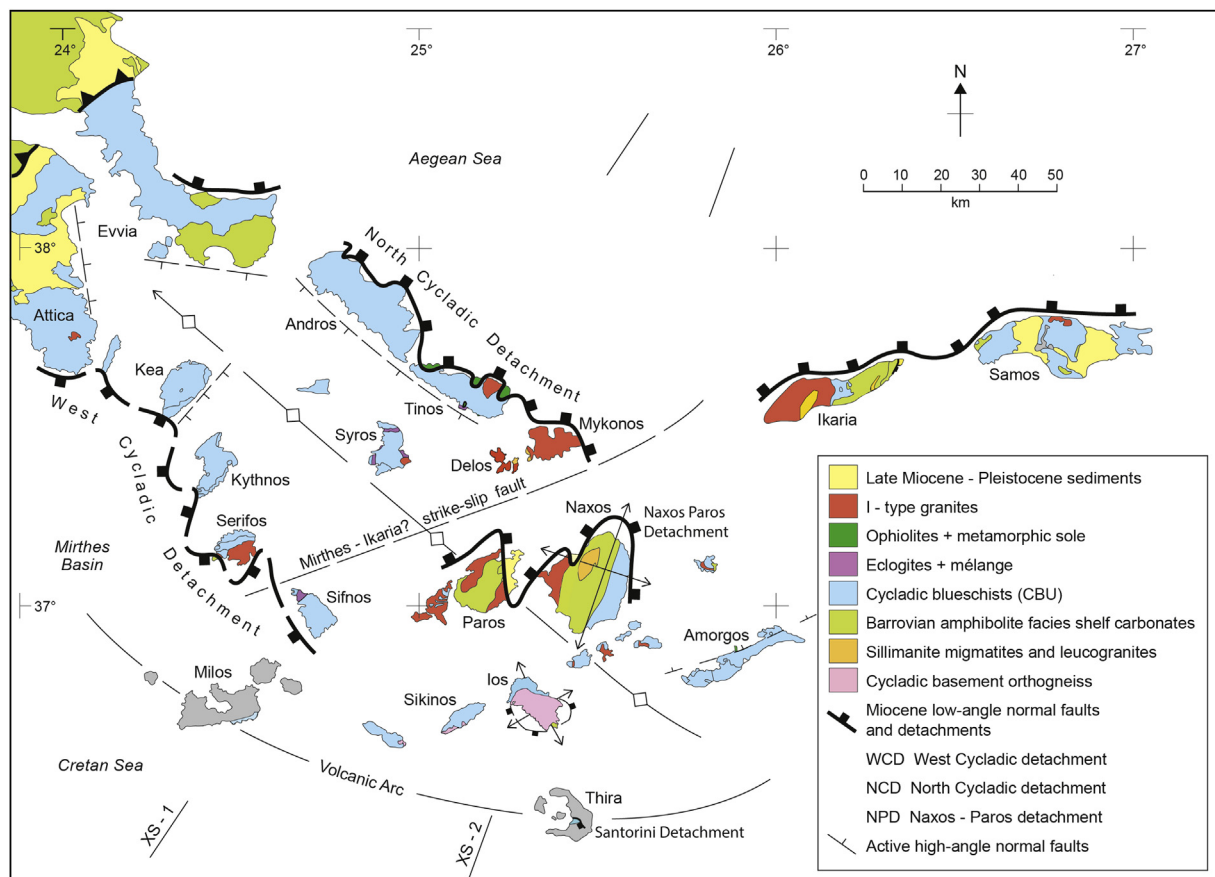


Fig. 2. Simplified geological map of the Cyclades islands, showing the main geological units together with three major extensional ductile shear zones, the North Cycladic Detachment (NCD), West Cycladic Detachment (WCD) and the Naxos-Paros Detachment system. Lines of cross-section on Fig. 3 are shown.

crustal thickening and extrusion processes (channel flow; Lamont et al., 2019; Searle and Lamont, 2019) rather than regional lithospheric Aegean extension.

In this paper, we discuss the structures across the Cyclades islands at all structural levels as well as the ‘extensional’ fabrics previously frequently related to orogenic collapse and regional lithospheric extension. We find that at least three different types of ‘extensional’ structures are present. Firstly, extensional fabrics in the Cycladic Blueschists are related to exhumation in a subduction channel in a compressional environment. Many HP rocks show isoclinal folding, thickening, and compressional structures associated with thrusting of eclogites over blueschists, over greenschist facies rocks, or rocks that did not reach as high pressures (Xypolias et al., 2003, 2012; Huet et al., 2009; Aravadinou and Xypolias, 2017; Laurent et al., 2018; Gerogiannis et al., 2019; Searle and Lamont, 2019; Lamont et al., 2020b; Ring et al., 2020). Secondly, extensional fabrics in core complex rocks are related to crustal thickening, regional metamorphism and exhumation beneath a fixed or passive roof fault (e.g. Koronos-Zas shear zones on Naxos, or the Vari detachment on Syros). These passive roof faults (Means, 1989) relate to ductile exhumation of footwall rocks beneath a stationary hanging-wall, in much the same way as the South Tibetan detachment low-angle normal faults along the northern Himalaya form the roof fault of the extruding middle crust rocks (channel flow; e.g. Searle, 2010, 2015). Thirdly, extensional fabrics along the major low-angle normal faults (e.g. NCD and WCD systems) which are related to regional crustal-lithospheric extension (e.g. Jolivet et al., 2009a, 2009b, 2010; Jolivet and Brun, 2010; Grasemann et al., 2012). Whereas Jolivet et al., (2009a, 2009b, 2010) proposed that the NCD started in the Oligocene concomitantly with Aegean extension, and Grasemann et al. (2012) and Ring et al. (2011) proposed that the WCD was active throughout the Miocene, we propose

here that regional Aegean extension was initiated at 15 Ma, and that earlier $^{40}\text{Ar}/^{39}\text{Ar}$ and U-Th/He ages are related to exhumation during earlier compressional tectonic events. None of the low-angle ductile shear zones or normal faults on the Cyclades islands appear to be active now. In fact, many islands (e.g. Naxos, Tinos, Ios, Sifnos) show very young uplift, doming and folding of the low-angle normal faults, indicating a Quaternary period of post-extension W-E shortening.

2. Extensional fabrics in a compressional environment

Ductile shear zones and mylonites generally develop several foliations that can provide good kinematic indicators or shear sense indicators. During progressive deformation foliations usually rotate from orientations showing active shortening to orientations that show extension and stretching (e.g. Hanmer and Passchier, 1991). Platt and Vissers (1980) used the terms compressional crenulation cleavage and extensional crenulation cleavage for shear band cleavage. Shear band cleavages develop by stretching during non-coaxial flow and form two planar fabrics, C and C' (Passchier and Trouw, 1996). C' type shear bands develop oblique to the shear zone boundaries and late in the strain history of the shear zone. C/S fabrics (cisaillement/schistosité in French) reflect inhomogeneous simple shear, and show a sense of shear generally recorded as ‘top-to-direction’ in the vertical plane, or dextral/sinistral in the horizontal plane. In many thrust belts, however, the motion is mainly recorded in the footwall rocks, leading to controversies such as the relative importance of hangingwall ‘collapse’ or footwall uplift. The simple geometry of the foliations provides evidence of relative motions of footwall and hangingwall rocks, not of overall constrictional or extensional strain.

Although microstructures and kinematic indicators record

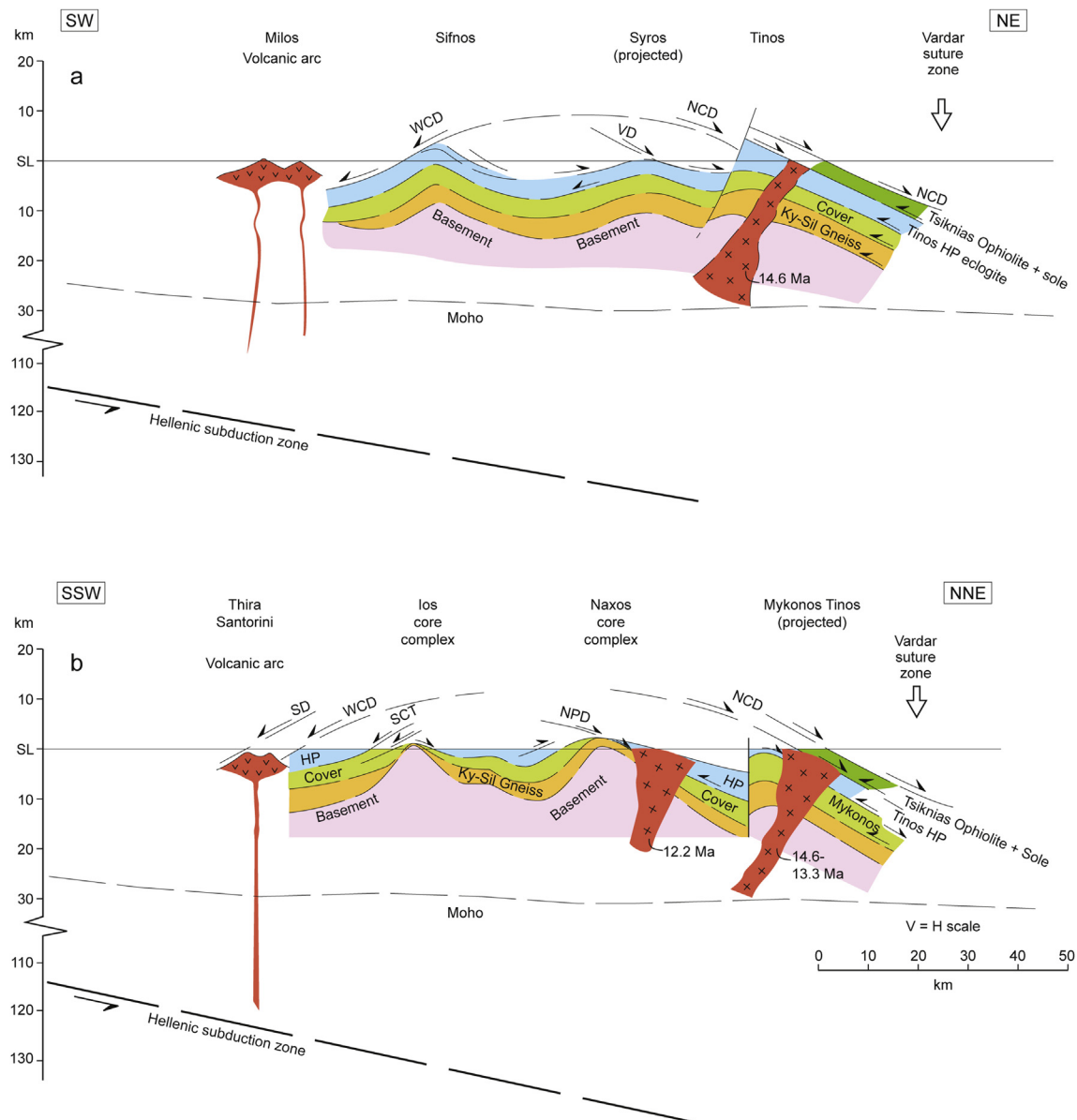


Fig. 3. Generalised cross-sections across the Cyclades islands (location of sections shown on Fig. 2) showing structural positions of the main core complexes in Naxos (+Paros), Tinos and Ios, with the overlying Cycladic Blueschist and HP eclogite unit (Zas unit on Naxos, Tinos, Syros and Sifnos HP units), and metamorphosed Mesozoic shelf carbonates in the Koronos unit and Naxos core unit.

extensional shear fabrics, they occur in zones of both overall crustal shortening and extension, and they record the relative uplift and exhumation of material, rather than a specific tectonic stress regime. 'Extensional' kinematic indicators or microstructures typically form via one of three geodynamic mechanisms: (1) buoyancy-driven extrusion of crustal material transported to depth within a subduction zone, which occurs under a passive-roof normal fault on the interface between the subducting slab and overlying mantle wedge, in conditions responsible for creating extensional fabrics in blueschists and eclogites (e.g. England and Holland, 1979; Hacker and Gerya, 2013); (2) exhumation and extrusion of high-grade migmatites and gneisses from a deep crustal root by coeval movement of a thrust at the base and an extensional synorogenic normal fault at the top, a mechanism called channel flow (e.g., the top of the GHS beneath the South Tibetan Detachment System (STDS); Law et al., 2006; Searle et al., 2006; Xypolias and Kokkalas, 2006; Ring et al., 2020); or (3) normal faulting during crustal extension and rifting (e.g., Wernicke, 1981; Wernicke and Burchfiel, 1982; Lister et al., 1984; Wernicke and Axen, 1988; Teyssier and Whitney, 2002; Jolivet et al., 2009a,b, 2009b).

Mechanisms 1 and 2 occur in compressional tectonic settings, while mechanism 3 occurs in crustal or lithospheric extensional settings. We believe that all three processes occur in the Cyclades at various stages throughout the Aegean orogeny. This is because the fabrics related to mechanisms 1 and 2 are folded by compressional stresses and truncated by ductile-brittle fabrics and structures related to regional extension (mechanism 3; e.g. western Naxos NPD; Lamont et al., 2019). We argue that normal sense fabrics (e.g. 'extensional crenulation cleavage', extensional C' shear band cleavage, etc.) in the Aegean and other mountain belts should be re-examined, as they cannot necessarily be used to independently relate to overall lithospheric extensional tectonism.

3. Regional tectonic setting

The tectonics of the Eastern Mediterranean is dominated by the convergence between the Africa (Nubia) plate and Eurasia, and the subduction of oceanic lithosphere in the southern Mediterranean northwards along the Hellenic trench and subduction zone, south of

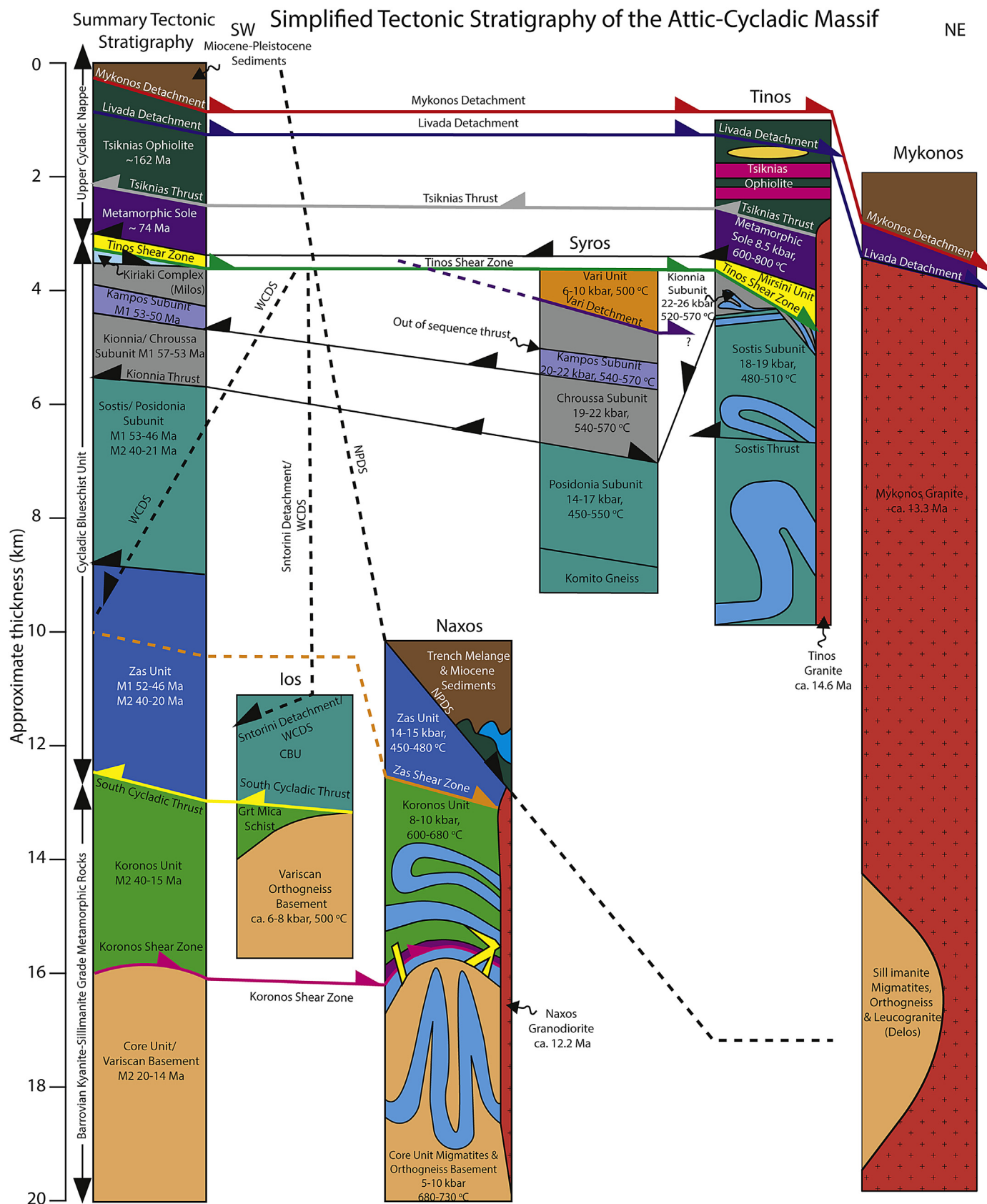


Fig. 4. Generalised tectonic-stratigraphic column for rocks from the Cyclades Islands, and individual columns for the islands of Ios, Naxos, Syros, Tinos and Mykonos, showing major tectonic units and main ductile shear zones, detachments and low-angle normal faults.

Crete (Fig. 1). Present-day Africa (Nubia) – Eurasia convergence is $\sim 5\text{--}10\text{ mm/yr}$ and Mediterranean oceanic crust subducts northward along the Hellenic trench at a rate of $\sim 35\text{ mm/yr}$ (Reilinger et al., 2006). The Hellenic subduction zone is largely aseismic with only a few large earthquakes taking up less than 20% of the strain (Shaw and Jackson, 2010). The overriding Aegean region is a complicated region including the southern extension of two suture zones (Pindos and Vardar sutures), a forearc, volcanic arc, a relatively aseismic Cyclades islands and the Northern Aegean back arc showing widespread N–S extension and NE–SW aligned dextral strike-slip faults (Jolivet and Brun, 2010). Recent earthquakes suggest that extension is concentrated mainly in the Northern Aegean and on the mainland, rather than in the central Aegean region around the Cyclades islands (Shaw and Jackson, 2010; Kapetanidis and Kassaras, 2019). GPS data shows the present-day motion of Aegean crust by $\sim 30\text{ mm/yr}$ towards the SW (McKenzie and Jackson, 1983; Billiris et al., 1991; McClusky et al., 2000; Floyd et al., 2010; Nocquet, 2012).

The major tectonic regions and processes involve: (1) the African (Nubian) plate which is converging north at rates of $0.5\text{--}1\text{ cm/year}$ with respect to the Aegean and Anatolian plates; (2) the Hellenic trench and

subduction zone, which shows a shallow north-dipping zone of earthquakes along which oceanic lithosphere subducts northwards beneath the islands of Crete and Cyprus; (3) a fore-arc region in the Cretan Sea stretching from the Peloponnese through Crete to Rhodes, which shows high seismicity levels; (4) an arcuate Quaternary volcanic arc stretching from SW Greece through Milos, Santorini and Astypalaia islands to the SW Turkey mainland; (5) a back-arc region in the Cyclades islands and Aegean Sea region, which shows few earthquakes; (6) the Northern Aegean back-arc basin, and Anatolian plate which is affected by E–W extension at $\sim 24\text{ mm/yr}$, and dextral strike-slip faulting, bounded along the north by the right-lateral North Anatolian strike-slip fault (Fig. 1).

The crustal structure of the Cyclades Islands (Figs. 2 and 3) in the Aegean Sea (zone 5) today is superficially dominated by structures related to regional scale extension. Older inactive extensional faults, including low-angle normal faults and widespread ‘extensional’ fabrics and kinematic indicators in the surface geology, are usually inferred to be related to deeper and earlier parts of the regional Aegean crustal-lithospheric extension (Lister et al., 1984; Jolivet et al., 2010). In general terms the structurally deeper detachments are related to older exhumation of firstly HP eclogites and blueschists, and secondly HT

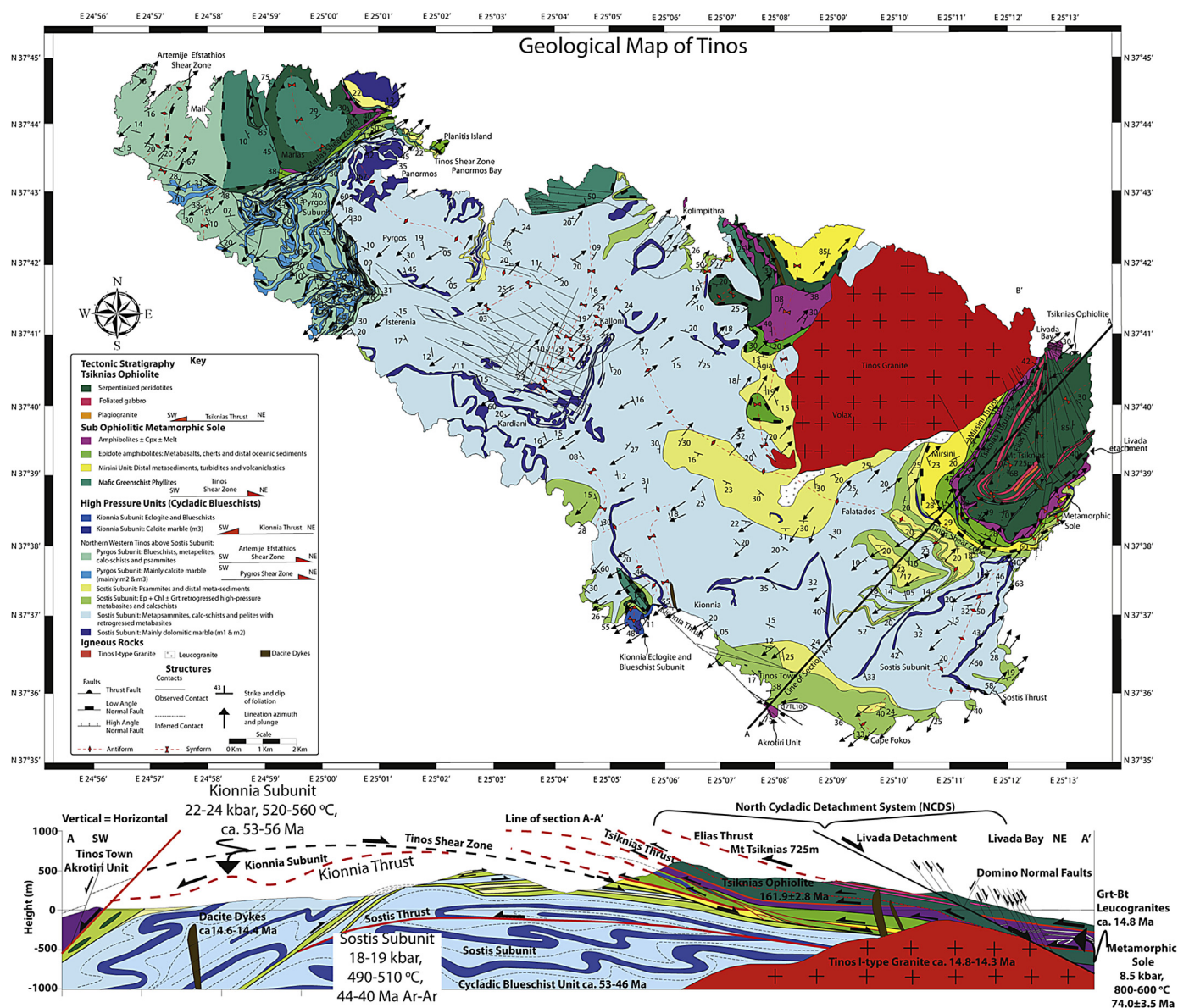


Fig. 5. Geological map and cross-section of Tinos island (after Lamont et al., 2020a, 2020b.).

sillimanite and kyanite grade gneisses. These older extensional shear zones sometimes merge upwards into and are truncated by the younger regional low-angle normal fault systems. Two major regional low-angle normal fault systems have been mapped and described extensively: (1) the **North Cycladic detachment (NCD)** system, extending from offshore Evia southeastward, and exposed along the north shores of the islands of Andros, Tinos, Mykonos (with an extension eastward to Ikaria and Samos) showing NE-directed extensional kinematic fabrics (e.g. Jolivet et al., 2009a, 2009b, 2010; Jolivet and Brun, 2010; Menant et al., 2016), (2) the **West Cycladic detachment (WCD)** system, exposed on Attica and the SW Cyclades islands of Kea, Kythnos and Serifos, showing consistent top-SW kinematics (Grasemann et al., 2012; Coleman et al., 2019). Other low angle normal fault systems include the **Naxos-Paros detachment (NPD)** on Naxos and Paros with top-NNE kinematics (Buick and Holland, 1989; Urai et al., 1990; Lamont et al., 2019), and the **Santorini Detachment (SD)** with top-south shear senses (Schneider et al., 2018). All the detachment systems were active at around the same time up until late Miocene, but show opposing shear sense directions on the NE and SW margins of the Cyclades dome. A cross-section across the Cyclades (Fig. 3) shows a major domal axis orientated NW–SE separating these two major shear zones. Islands within the central part of the Cyclades (Naxos, Paros, Ios) show the deeper structural levels where metamorphic core complexes show HT-MP (kyanite, sillimanite grade) rocks in the core zone and even Cycladic basement rocks on Ios, Naxos and Paros. The island of Tinos shows a complete profile across the ophiolite and HP Cycladic Blueschist Unit (Fig. 5, after Lamont et al., 2020a, 2020b). The island of Syros shows the most complete profile across the HP and UHP rocks of the Cyclades (Fig. 6). The island of Naxos shows the most complete section from the structurally higher Cycladic Blueschist Unit through the kyanite and sillimanite grade rocks of the Naxos metamorphic core complex (Fig. 7, after Lamont et al., 2019). Tinos and Naxos islands both have young granite intrusions, whose ages can be used to constrain timing of shear fabrics in the ductile shear zones.

4. Aegean orogeny, geology of the Cyclades archipelago

Eight stages are recognised within the Aegean orogeny following a classic Wilson cycle from early ophiolite obduction onto a previously passive continental margin to attempted crustal subduction with HP metamorphism (eclogite, blueschist facies), through crustal thickening and regional Barrovian-type metamorphism (kyanite, sillimanite grade), to orogenic collapse. Each stage is schematically depicted in Fig. 8 together with U–Pb geochronological constraints and the corresponding P–T–t paths for rocks formed at these times.

The **early** parts of the Aegean orogeny are recorded by:

- (1) SW-directed obducted ophiolite complexes (e.g. Tsiknias Ophiolite), and the underlying amphibolite – greenschist facies metamorphic sole (Jolivet et al., 2015; Lamont et al., 2020a, 2020b)
- (2) Subducted and then exhumed eclogites and blueschists at ~54–40 Ma best exposed on Syros, Sifnos, Tinos, Ios and Naxos islands (Trotet et al., 2001; Tomaschek et al., 2002; Keiter et al., 2004, 2011; Lagos et al., 2007; Ring et al., 2007, 2020; Philippon et al., 2011, 2012; Soukis and Stockli, 2013; Roche et al., 2016; Laurent et al., 2016, 2016b, 2018; Lamont et al., 2020a, 2020b). Fig. 9 shows the tectonic positions of each unit at this time, prior to the regional kyanite and sillimanite grade metamorphism of Koronos and core units on Naxos.

The **later** parts of the Aegean orogeny are recorded by:

- (3) Crustal thickening and shortening within the sedimentary cover rocks, dominantly shelf carbonates, up to kyanite grade P–T conditions best seen on Naxos, Tinos, Andros, Sifnos (Lister et al., 1984; Urai et al., 1990; Keay et al., 2001; Kruckenberg et al., 2011; Rey et al., 2011, 2017; Lamont et al., 2019).

- (4) Deep crustal core complexes formed by E–W compression and constriction, with upright tight – isoclinal folding under sillimanite-grade metamorphic conditions, with partial melting resulting in S-type leucogranites (Naxos; Buick and Holland, 1989; Urai et al., 1990; Kruckenberg et al., 2011; Rey et al., 2011, 2017; Lamont et al., 2019).
- (5) Intrusion of coeval I-type granites (e.g. on Naxos, Paros, Tinos, Mykonos, Serifos) and minor S-type leucogranites emanating from a central migmatite core (e.g. Naxos, Delos, Tinos) at 17–13 Ma (Keay et al., 2001; Brichau et al., 2007; Iglseider et al., 2009; Beaudoin et al., 2015; Rabailard et al., 2018).

The final parts of the Aegean orogeny are recorded by:

- (6) Regional low-angle normal faults and detachments (<15 Ma) recording regional Aegean extension (Jolivet et al., 2010; Jolivet and Brun, 2010). The South (or West) Cycladic detachment (Ring et al., 2007, 2011; Grasemann and Petrakakis, 2007; Grasemann et al., 2012; Coleman et al., 2019) shows top-to-SW shear fabrics and low-angle normal faults on the islands in the SW Cyclades (Serifos, Sifnos, Sikinos). A second structurally higher south-dipping detachment is present on Santorini island, the Santorini detachment system (Schneider et al., 2018). The North Cycladic detachment (Jolivet et al., 2010) dips to the NE and is exposed around the northern coasts of the north Cycladic islands (Andros, Tinos, Mykonos, and Paros, Naxos). Timing constraints indicate a continuum of deformation from ductile low-angle shearing to brittle cataclasis, both with structural depth and time.
- (7) Large scale NE–SW contraction forming a ~100 km wavelength dome along the central Cyclades. Deeper structural levels are seen along this anticline axis in the islands of Paros, Naxos and Ios, where core complexes show metamorphosed, mainly Variscan orthogneissic basement (Ios) and mainly paragneiss cover (Naxos, Tinos, Sifnos) units folded about NNE–SSW or WNW–ESE fold axes with compressional upright folds in the core (Lamont et al., 2019; Searle and Lamont, 2019). The low-angle detachments, normal faults, and fluvial sediments that formed during stage 6 are folded around these fold axes clearly indicating a period of post-extension ENE–WSW compressional doming (Lamont et al., 2019). Much of the high and steep topography on the Cycladic islands is a combined result of this period of shortening followed by normal faulting around the flanks.
- (8) Fault plane solutions and earthquakes in the Aegean region clearly show present-day NE–SW extension across the northern Aegean Sea region. Earthquakes in the Corinth–Patras rift nucleate along the Pleistocene-active low-angle (20°) normal fault, above which higher angle normal fault show a cumulative extension of 15 km (Sorel, 2000). Steeper normal faults across the Cyclades typically splay off a major, regional low-angle detachment (Jolivet et al., 2010). Santorini volcano lies in a NE–SW aligned graben bounded by steep active normal faults south of Ios and Amorgos islands. The 1956 Amorgos Mw 7.5 earthquake was related to N–S extension along the volcanic arc south of Ios and Amorgos islands, and not to tectonics of the back-arc Cyclades (Papazachos, 2019). The geomorphology of most islands in the Cyclades shows a relatively high topography, steep slopes indicative of a recent high uplift rate, and drowned coastlines indicative of Quaternary tilting and subsidence (e.g. particular the north coasts of Tinos and Andros).

5. Ophiolite formation and obduction (Tinos)

The Tsiknias Ophiolite is exposed on the northern coastline of Tinos and is the highest exposed thrust sheet in the Cyclades (Fig. 5). It comprises a 700-m thick section of mafic and ultramafic mantle and lower crustal oceanic rocks including massive serpentinised harzburgites,

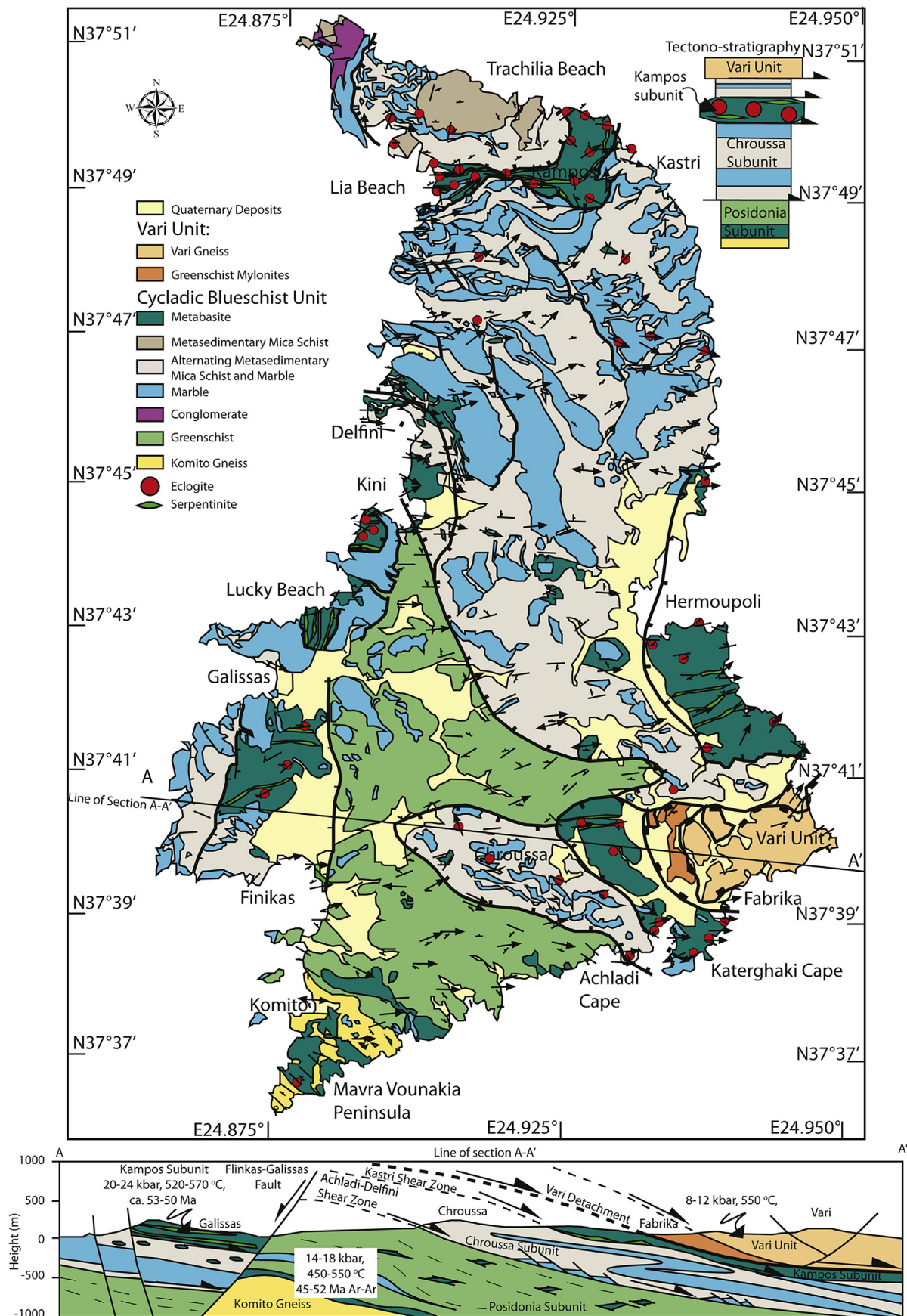


Fig. 6. Geological map and cross-section of Syros island, simplified after Keiter et al. (2004, 2011), Philippon et al. (2011, 2012), Laurent et al. (2016, 2018) and our own observations.

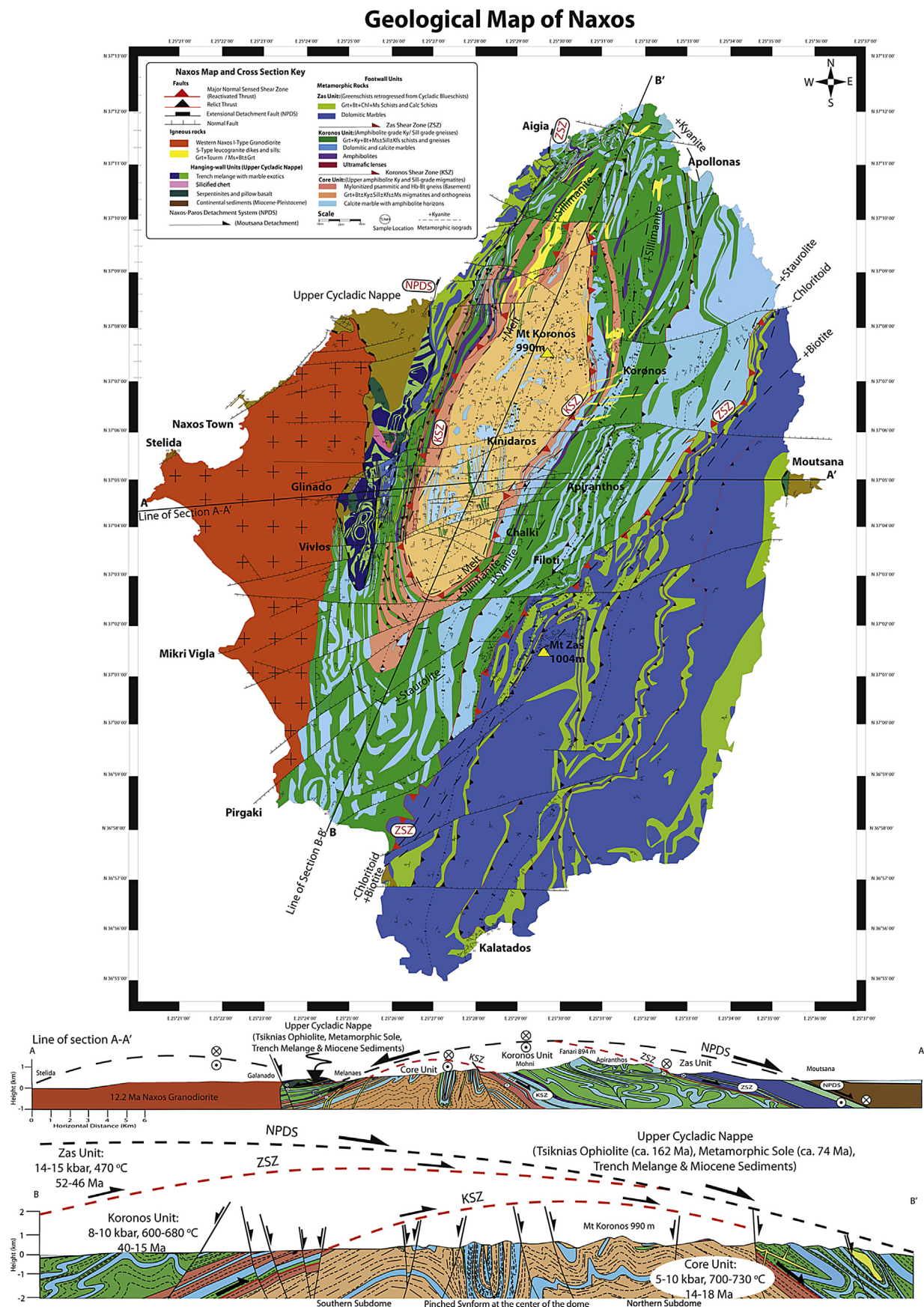


Fig. 7. Geological map and cross-sections of Naxos island (after Lamont et al., 2019).

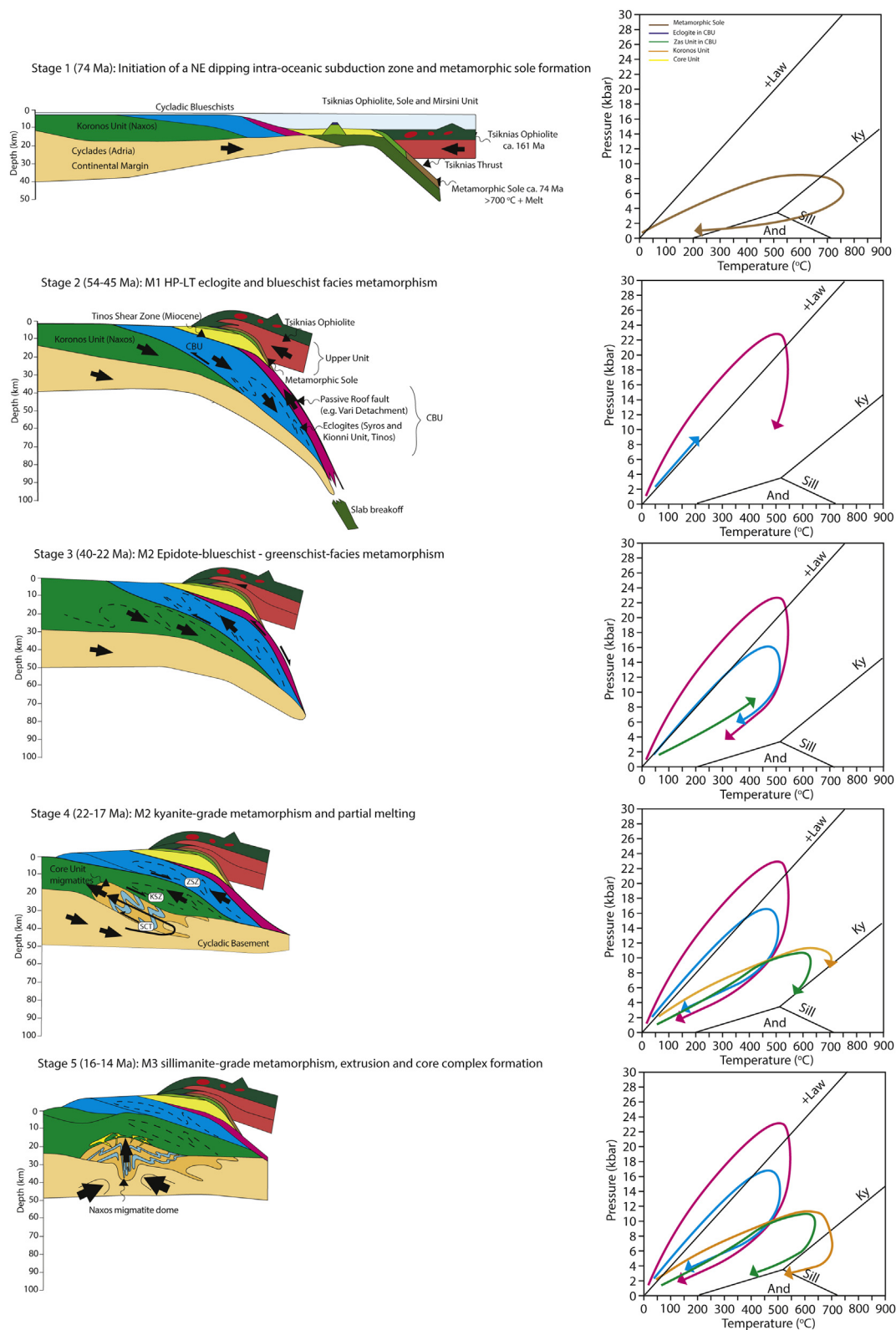


Fig. 8. Sequential tectonic evolution diagrams for the Aegean Orogeny with sketch P-T-t paths for the various units involved with each stage of the orogeny. Stage 1: Ophiolite obduction and formation of the metamorphic sole. Stage 2: Subduction of the leading edge of the NE Adrian passive margin to eclogite facies conditions (Kini and Lia mélanges on Syros, and Kionnia Unit on Tinos). Stage 3: Continued subduction and underplating of the more proximal Adrian passive margin to blueschist facies conditions (Zas Unit on Naxos; interior of Sifnos), whilst the earlier buried rocks were experiencing exhumation due to their positive buoyancy. Stage 4: Burial of the proximal passive margin under a warmer geotherm to kyanite grade conditions as a result of crustal thickening (Koronos and Core Units on Naxos). Stage 5: Partial melting and NE-directed extrusion of the Koronos and Core Units resulting in muscovite dehydration melting and sillimanite grade metamorphism. Followed by low-angle normal faulting (NCDS, NPDS and WCDs) coeval with I-type granite intrusion that cut the earlier collisional features and 'extensional' fabrics.

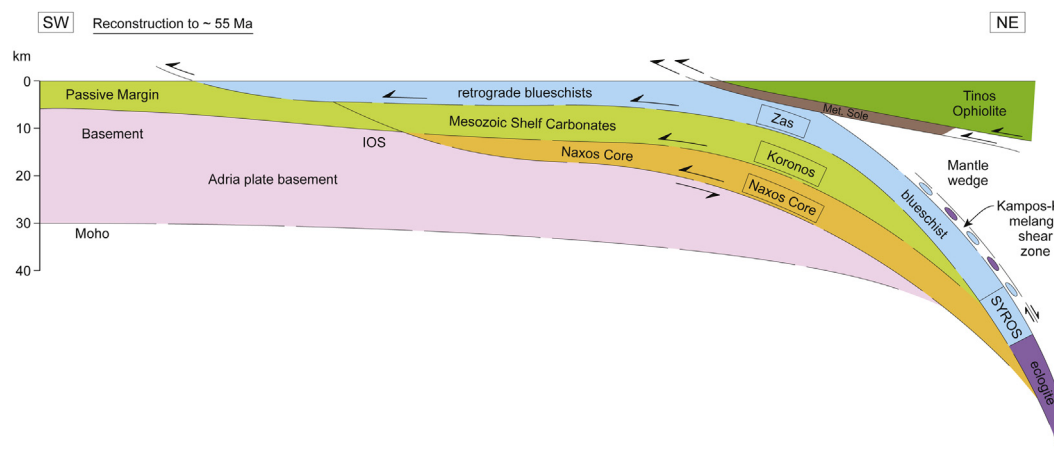


Fig. 9. Reconstruction of the Adria passive continental margin to ~55 Ma during the beginning of subduction and HP metamorphism in the Cycladic blueschist-eclogite unit, and prior to the regional kyanite- and sillimanite grade metamorphism in the Koronos and Naxos core units, showing the relative positions of each major structural unit.

dunites and intercalated foliated gabbros and plagiogranite sills representative of the Moho Transition Zone. The upper crustal parts of the ophiolite (sheeted dykes, pillow lavas) are not preserved. U–Pb geochronology of a large plagiogranite sill constrains the timing of magmatism associated with SSZ spreading as ca. 162 Ma, which was followed by intrusion of numerous gabbros that show variable subduction signatures at ca. 145 Ma (Lamont et al., 2020a). A ~300 m thick section of amphibolite and greenschist facies metamorphic sole rocks underlying the ophiolite on Tinos (Fig. 10a and b), record SW-directed thrusting and isoclinal folding associated with ophiolite emplacement. The amphibolites represent meta-basalts and meta-gabbros that formed at ca. 190 Ma before being buried and metamorphosed to P–T conditions of ca. 8.5 kbar and 600–800 °C and underwent partial anatexis at ca. 74 Ma along the interface of a newly formed NE-dipping intra-oceanic subduction zone (Lamont et al., 2020a). These ages reveal the Tsiknias Ophiolite formed to the NE of Tinos in present day co-ordinates in the Vardar Ocean and remained as an intact piece of oceanic lithosphere for ca. 90 Myr. It was only at ca. 74 Ma that a new NE-dipping intra-oceanic subduction zone initiated (Fig. 8, stage 1) due to the Africa (Nubia) plate motion possibly changing from transcurrent (E–W) to convergent (N–S) (Vissers and Meijer, 2012). U–Pb zircon ages of 63 Ma and 61 Ma from a jadeitite in Tinos (Bröcker and Enders, 1999) may reflect the transition from ophiolite obduction to subduction of the continental margin on Tinos, although another U–Pb age of ca. 53 Ma from a glaucophanite on Tinos may suggest this older age is a mixed age (Bulle et al., 2010).

During this subduction initiation event, the zone of active thrusting stepped down section through time, resulting in underplated material including pelagic metasediments being accreted to the base of the ophiolite. On Naxos, in the hangingwall of the Naxos-Paros Detachment (NPD), there is evidence for limestone exotic blocks in a mélangé, bounded by serpentine and metabasalts that represent a thrust sheet of trench mélangé associated with subduction of a seamount similar to the Haybi Complex beneath the Oman Ophiolite (Searle et al., 1994). NE-dipping subduction continued between ca. 74–53 Ma when the leading edge of the Cycladic continental margin arrived at the trench, resulting in attempted subduction of the continental margin and HP metamorphism (see below).

6. Eclogite – blueschist subduction and exhumation (Tinos, Syros, Sifnos)

The Cycladic Blueschist Unit (CBU) is exposed laterally NE–SW over >80 km across the Cyclades and is exposed at intermediate structural levels on every island (Fig. 4). The CBU represents a series of tectonically

bound slices of oceanic crustal material and continental margin rocks that experienced eclogite to blueschist facies conditions (Trotet et al., 2001; Tomaschek et al., 2002; Keiter et al., 2004, 2011; Lagos et al., 2007; Philippon et al., 2011, 2012; Soukis and Stockli, 2013; Roche et al., 2016; Laurent et al., 2016a, 2016b, 2018; Lamont et al., 2019, 2020b; Ring et al., 2020). At structurally high levels, a series of mélanges are exposed (Kampos and Kini in north and west Syros respectively), which include HP–LT mafic eclogites and lawsonite-bearing blueschists (Keiter et al., 2004, 2011). North of Galissas on the west coast of Syros a spectacular ophiolite mélangé zone (Kampos Subunit) is exposed (Fig. 10c), composed of eclogite and blueschist facies banded meta-gabbros (Fig. 10d and e) bounded by serpentinised harzburgites with enstatite, talc and kosmochlore, a chromium-rich pyroxene (Fig. 10f). This eclogite facies unit has strongly folded meta-carbonates on both sides (Chroussa and Pyrgos subunits marbles and schists). Within these mélangé zones, meta-basic eclogites and blueschists are both gabbroic and doleritic, and occur together with Mn-rich meta-cherts (spessartine + piemontite + quartz), marbles and quartzites and larger coherent meta-volcaniclastic blocks/horizons which are enclosed in a serpentine matrix.

Meta-basic eclogites contain glaucophane, garnet, lawsonite pseudomorphs, omphacite, phengite, paragonite and epidote (Fig. 11a,b,c). Coarse-grained meta-gabbros contain green kosmochlore, omphacite and plagioclase. Both probably represent metamorphosed ophiolitic rocks that yielded U–Pb magmatic crystallization ages of 78 ± 1 Ma from an omphacite-bearing eclogite (Bröcker and Enders, 1999, 2001) and ca. 77 Ma (Tomaschek et al., 2002; Bröcker et al., 2014; Hinsken et al., 2016). The boundary of the Kini mélangé in western Syros is a 20 m-wide highly deformed ductile shear zone within serpentinised harzburgite or dunite. Thicker banded calc-schists and marbles derived from the Mesozoic shelf carbonates wrap around the top of the Kini and Kampos mélanges suggesting they have been emplaced into the shelf carbonate sequence by out-of-sequence thrusting during the exhumation process. Both HP eclogites and calc-schists are tightly folded and transposed into ductile shear zones. Tight to isoclinal folds in meta-chert bands representing the pelagic sediments overlying oceanic crust, are exposed in the Kampos shear zone (Fig. 11d,e,f). There is some debate as to the peak P–T conditions of the eclogitic rocks. Trotet et al. (2001) suggested P–T conditions of 15–20 kbar and 550 °C, whereas Laurent et al. (2018) suggested peak M1 conditions of ca. 19–22 kbar and 550 °C, by phase equilibria modelling. The timing of peak metamorphism based on Lu/Hf garnet geochronology is ca. 52 Ma (Lagos et al., 2007). Structurally underlying the HP mélanges, eclogites and blueschist are exposed as meta-volcanic clastic horizons within the leading edge of the Mesozoic shelf carbonate sequence (Chroussa subunit on Syros, and

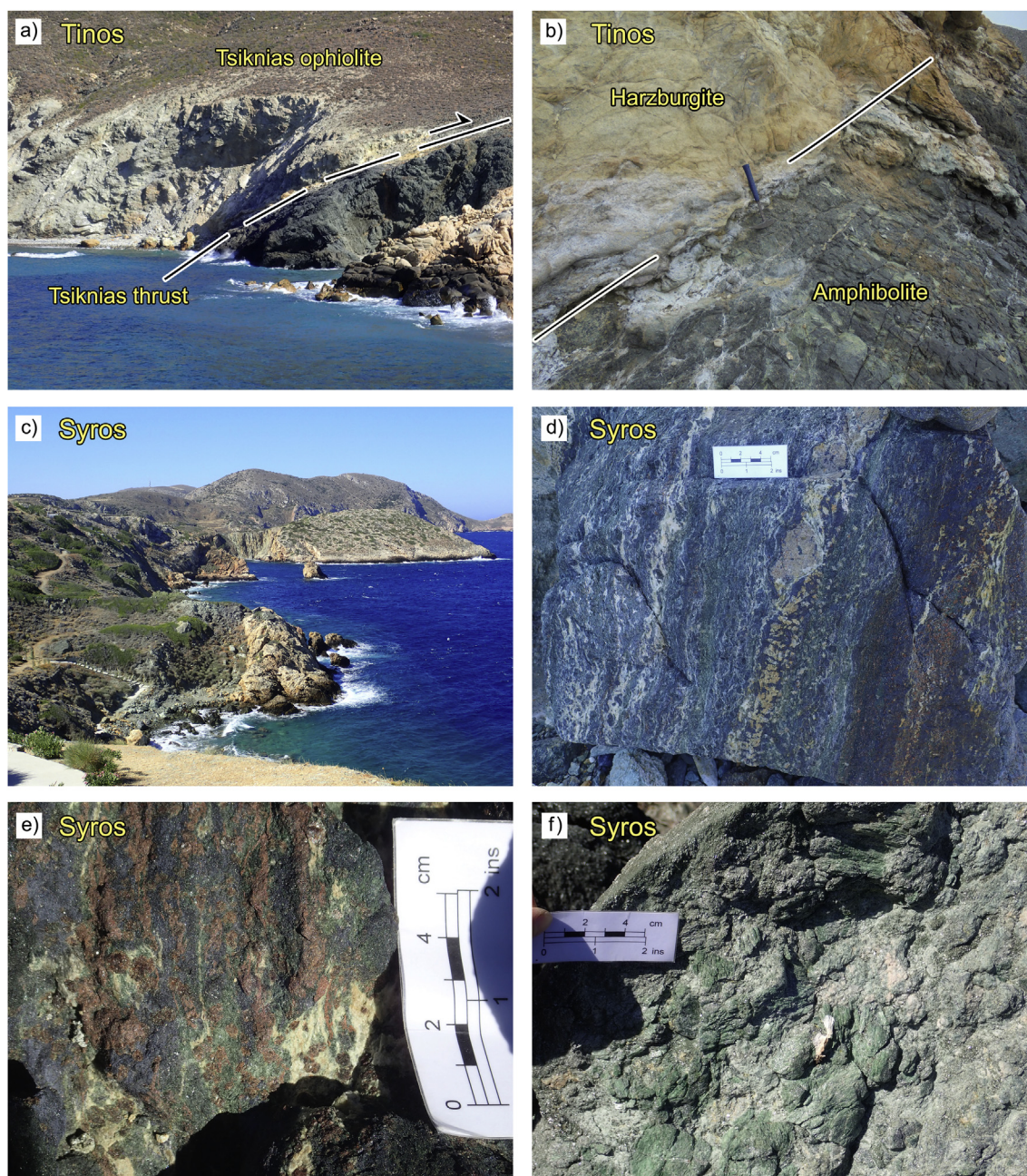


Fig. 10. (a) Base of the Tsiknias ophiolite with the ultramafic rocks thrust over amphibolites of the metamorphic sole, Livada Bay, Tinos. (b) Tsiknias thrust showing partial melting in the upper levels of the Metamorphic sole amphibolites, Livada Bay, Tinos. (c) View of the Kini – Galissas ophiolite mélange zone, with vertical serpentinite shear zones bounding eclogites and blueschists, with meta-carbonate units to west (right), west coast Syros. (d) Banded meta-gabbroic eclogites showing garnet + omphacite + glaucophane + pargasite/albite assemblage, Kini mélange zone, Syros. (e) Glaucophane + garnet + omphacite + plagioclase meta-gabbros, Kini mélange zone, Syros. (f) Green kosmochlore + plagioclase meta-gabbros, Kini mélange zone, Syros.

Kionnia and Pyrgos subunits on Tinos). On Tinos, the Kionnia sub-unit reached ca. 22–26 kbar and 520–560 °C, and was thrust towards the SW over rocks that did not reach as high pressure (18.5 kbar and 490 °C; Sostis subunit). These structurally deeper rocks (Sostis subunit on Tinos, Zas Unit on Naxos, interior of Sifnos) represent the more proximal sequence of the continental margin and are affected by more intense greenschist-amphibolite facies retrogression. They now represent albite + epidote retrograde blueschists and are dominated by greenschists. These rocks also yielded younger metamorphic ages of ca. 46 Ma on Sifnos (Lu/Hf garnet geochronology; Dragovic et al., 2012) and 52–46 Ma on Naxos (Lamont, 2018), whereas Rb–Sr yields ages of ca. 40 Ma (Peillod et al., 2017).

On Ios island Lister et al. (1984) and Vandenberg and Lister (1996)

mapped the lower contact of the Cycladic Blueschist Unit as a top-south extensional detachment. However, detailed mapping and fabric analysis by Huet et al. (2009) showed that this contact, placing HP eclogite-blueschists over basement rocks which did not experience HP, was a SW-directed thrust, active concomitantly with a syn-orogenic top-NE detachment along the top of the CBU, both active during the Eocene. This SW-extrusion of HP rocks concurs with the interpretation of return flow extrusion from the subduction channel (Laurent et al., 2016a, b; Lamont et al., 2020b; Ring et al., 2020) and from our interpretation of structures on Tinos and Syros.

Top-NE ‘extensional’ fabrics are extensive throughout the Cycladic Blueschist Unit, and are coeval with more localised top-SW thrust-related fabrics and isoclinal folding (Fig. 8, stage 2). Within the CBU on Tinos, at

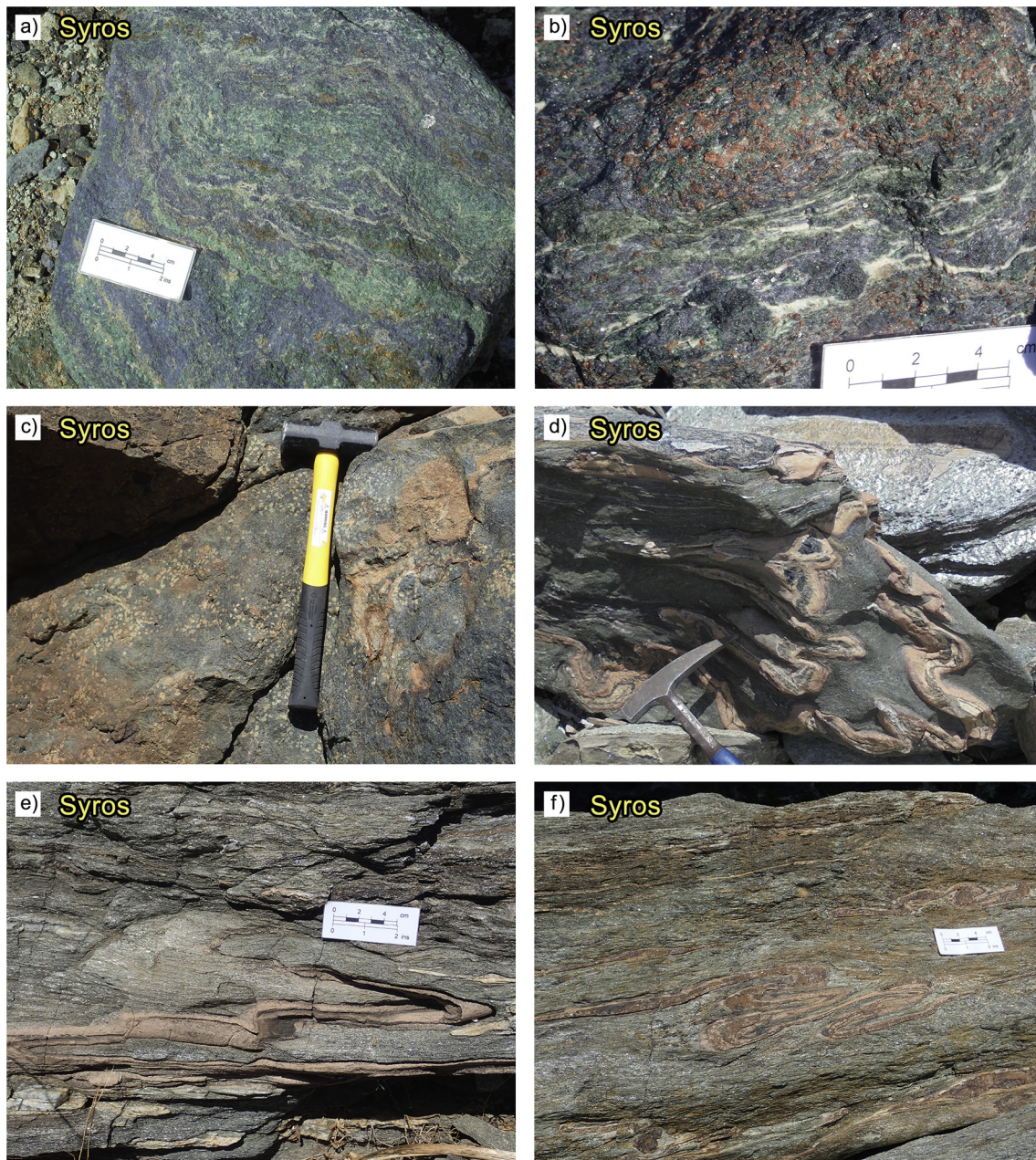


Fig. 11. (a) Glaucophane + omphacite meta-basalts, Kini mélange zone, Syros. (b) Coarse-grained garnet + omphacite + glaucophane + plagioclase meta-gabbros, Kini mélange zone, Syros. (c) Late euhedral lawsonite (pseudomorphed by clinozoisite, phengite, quartz, chlorite) crystals (white) showing static metamorphism overprinting the main UHP fabric, Lia beach, Syros. (d) Isoclinal compressional folding in Mn-rich *meta*-cherts interbanded with HP eclogites, Lia beach, Syros. (e) Tight folding in eclogites with banded *meta*-cherts, Lia beach, Syros. (f) Compressional folding with the HP eclogites, Lia beach, Syros.

least two distinct subunits have been identified which experienced contrasting tectono-thermal histories (Lamont et al., 2020b). An inverted metamorphic field gradient is observed across a zone of strong eclogite-blueschist facies top-SW shearing near Kionnia at high structural levels, suggesting the sequence represents a thrust placing more deeply buried eclogite and blueschist (22–26 kbar, 520–560 °C; Kionnia subunit) onto less deeply buried blueschists and greenschists (18 kbar, 480 °C; Sostis subunit). This thrust would have represented the base of a SW-directed exhuming subduction channel or wedge at eclogite facies depths (Lamont et al., 2020b). In contrast, within and at the top of the mélanges in Syros, top-NE shearing at peak eclogite and blueschist facies conditions represents the roof shear sense of the extruding channel or wedge, and the HP mafic rocks with the mélanges are overlain by continental margin rocks that did not reach as high pressure, consistent with

this idea (Fig. 8, stage 3). Consistent with this, (S)SW-directed shearing are also recorded in amphibolites and greenschists in the footwall rocks of the Vari detachment on Syros (Soukis and Stockli, 2013; Aravadinou and Xypolias, 2017). Unfortunately, due to later cross-cutting low-angle normal faults the upper half of the subduction channel or wedge is truncated (e.g. NCD cutting the Tinos HP rocks), where ca. 25 Myr of subduction history is missing (Lamont et al., 2020b). The HP rocks of the CBU are juxtaposed against the metamorphic sole rocks, with the age of juxtaposition being constrained by the regional greenschist event at ca. 21–23 Ma (Bröcker et al., 1993; Bulle et al., 2010).

On Milos, located in the hangingwall of the West Cycladic Detachment, another subunit at the structurally highest part of the CBU has been identified (Grasemann et al., 2017). The Kiriaki complex (basement on Milos) experienced ~8.5 kbar and 400 °C and pervasive ductile

deformation in the Paleocene–Eocene, with top-to-S to -SW shearing (Grasemann et al., 2017). These P–T conditions are similar to rocks from the ‘Upper Tectonic Unit’ on Attica (Baziotis et al., 2020), that also lies structurally above the possible continuation of the West Cycladic

Detachment (Coleman et al., 2019; Baziotis et al., 2020). P–T conditions from exposed rocks Milos contrast with eclogite pebbles (xenoliths) within the green lahar unit that are derived from structurally deeper levels beneath Milos and attained P–T conditions similar to the rest of the

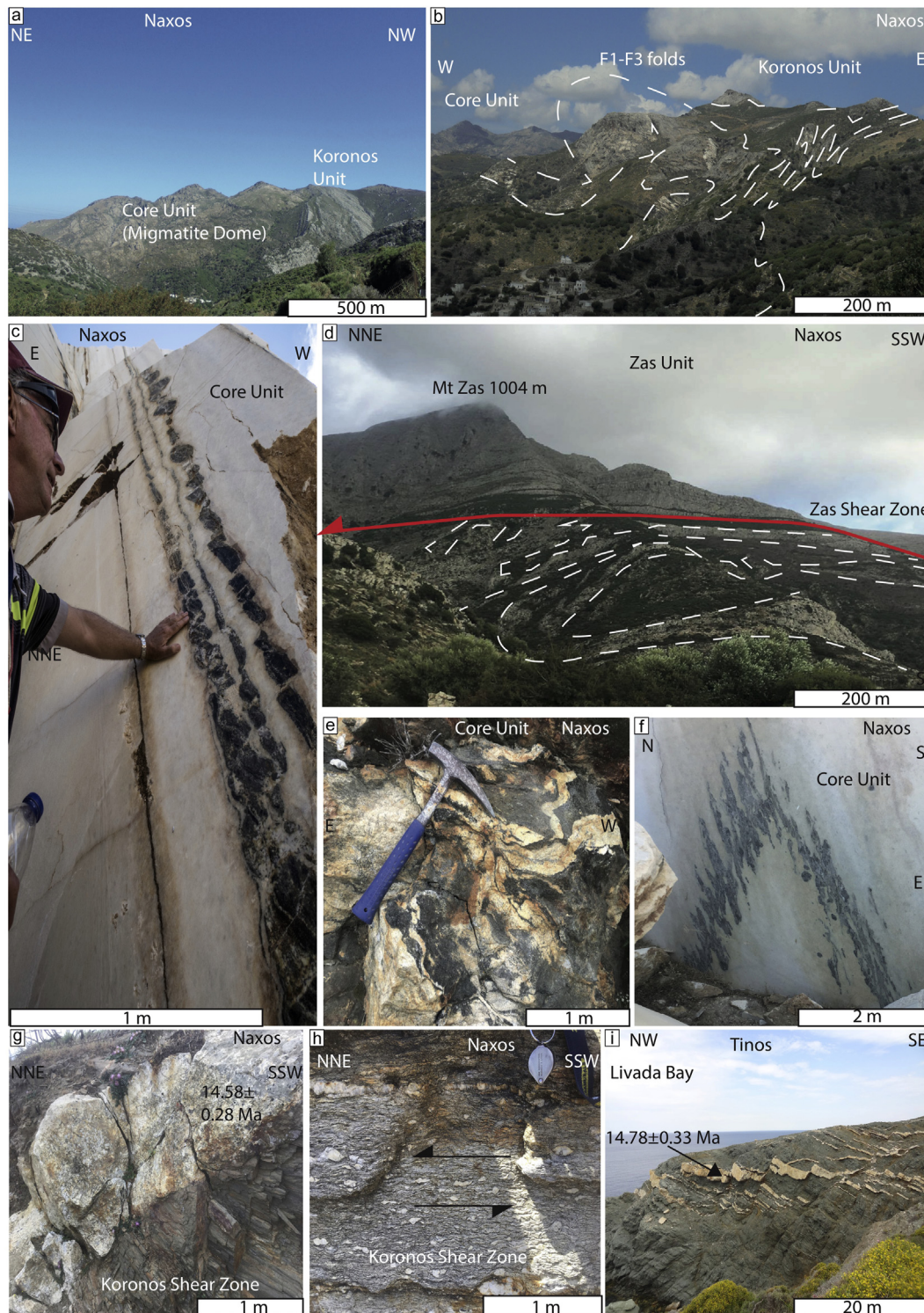


Fig. 12. (a) Core unit of the Naxos metamorphic core complex, (b) isoclinal folds in the Koronos unit in kyanite grade gneisses and marbles, above Filoti village, Naxos. (c) Vertical boudinage of amphibolite band within marble indicating horizontal constriction, Core unit of the Naxos core complex. (d) Panorama of the Zas shear zone separating retrogressed blueschist of the Zas unit above from kyanite grade gneisses of the Koronos unit below. (e) Diatexite migmatites of the Core unit, Naxos core complex. (f) Upright tight folding in amphibolite band within marble, Naxos Core unit. (g) Leucogranite dyke cross-cutting top-to-NE shear fabrics of the Koronos shear zone. (h) Blastomylonites in basement orthogneiss of the Koronos shear zone. (i) Domino normal faulting offsetting 14.78 Ma leucogranites, indicative of regional extension, Tinos.

CBU of ca. 19 kbar and 550 °C (Grasemann et al., 2017). The right way up metamorphic gradient at the top of the CBU and inverted metamorphic gradient at the base support the hypothesis that the CBU was sequentially extruded from the subduction zone and the sub-units became coupled at various depths during the exhumation process. This exhumation process was probably associated with a change in boundary conditions associated with continent-continent collision between Eurasia to the north and Adria-Apulia to the south.

7. Barrovian metamorphism and core complex formation (Naxos)

Following the oceanic subduction phase, post-collisional crustal thickening resulted in regional Barrovian metamorphism that affected the middle and lower crust levels of the Cyclades. The geodynamic history of regional-scale M2 kyanite- and M3 sillimanite-grade metamorphic rocks that are exposed within the core of the Naxos dome (Fig. 12a–g), a classic metamorphic core complex (Lister et al., 1984; Urai et al., 1990; Buick, 1991; Keay et al., 2001; Martin et al., 2006; Kruckenberg et al., 2011; Rey et al., 2011, 2017; Lamont et al., 2019). The origin of the metamorphic core of the Naxos dome is controversial. Most workers interpreted the origin of the migmatite core as buoyancy-driven flow or diapirism, driven by N–S extension (Lister et al., 1984; Rey et al., 2001, 2011; Teyssier and Whitney, 2002; Vanderhaege, 2004; Vanderhaege and Teyssier, 2001; Kruckenberg et al., 2011). However, Lamont et al. (2019) and Searle and Lamont (2019) noted that the mapped upright isoclinal folds in the core and vertical stretching lineations indicated compressional tectonics with significant amount of horizontal shortening and constriction, related to crustal thickening. The upright folds and stretching lineations are truncated along the upper margin by the later, low-angle detachment which wraps around the island in a circular map pattern. Furthermore, the normal sense fabrics are uni-directional (top-to-NNE) and folded about the migmatite dome, suggesting the doming post-dated the shearing and decompression. This is inconsistent with the buoyancy driven flow model, where a radial divergent shear sense pattern would be expected, due to the inflowing migmatites that are mechanically decoupled from the overlying crust. In our model, the migmatite dome within the core complex is formed by horizontal compression and uplift of footwall rocks prior to regional extension. Any extensional orogenic collapse occurred along normal faults that formed after peak metamorphism and isoclinal folding of the core.

The pre-extensional prograde evolution of these rocks and the relative timing of peak metamorphism in relation to the onset of extension is poorly known. Kyanite- and sillimanite-grade gneisses within the core complex record a complex history of burial and compression, and did not form under conditions of crustal extension (Fig. 8, stage 4). Deformation and metamorphism was diachronous, and propagated down-structural section with time, resulting in the juxtaposition of several distinct tectonostratigraphic nappes that experienced contrasting metamorphic histories. Thermobarometric studies show that the kyanite and sillimanite grade gneisses in the core of Naxos dome record crustal thickening and Barrovian metamorphism at ca. 40–15 Ma. These rocks underwent a clockwise P–T evolution and resulted in M2 kyanite-grade conditions of ca. 10 kbar and 600–670 °C, between 22 Ma and 17 Ma (Lamont, 2018; Lamont et al., 2019). At the deepest levels, kyanite-grade, fluid-fluxed melting at ca. 8–10 kbar occurred between 18.5 Ma and 17 Ma, and was followed by isothermal decompression and sillimanite-grade, fluid-absent dehydration melting (ca. 5–6 kbar and 730 °C) at 16–14 Ma, facilitated by exhumation under a series of top-NNE passive roof normal faults (Fig. 4). The migmatite dome formed at lower pressure conditions under horizontal constriction resulted in vertical bouinage and upright isoclinal folds, that refold the ductile shear zones (Fig. 8, stage 5).

U–Pb dating of zircons from leucogranite dykes that cross-cut and therefore post-date the shear zones (Fig. 11g), combined with young ages from sillimanite-grade gneisses constrain the timing of top-to-NNE

shearing along these shear zones to 18–15.5 Ma, corresponding to an average exhumation rate of 6 km/Myr (Lamont et al., 2019). These structures pre-date doming and are responsible for southwest directed extrusion of gneisses and migmatites from 35 to 17.5 km depth in a compressional setting (Lamont et al., 2019; Searle and Lamont, 2019). The rocks were subsequently folded around the central migmatite dome on Naxos. During this sillimanite grade metamorphic event, muscovite dehydration melting produced S-type garnet tourmaline and biotite-muscovite leucogranites (Fig. 12e), dated at ca. 18–13 Ma on Naxos, that cross-cut the overlying top-NE shear zones (Keay et al., 2001; Beaudoin et al., 2015; Lamont, 2018). Similar leucogranites also occur on Tinos and Delos and intrude coeval with, or immediately prior to, adjacent I-type granitoids (ca. 15–11 Ma; Brichau et al., 2007; Iglseder et al., 2009; Beaudoin et al., 2015; Lamont, 2018).

8. Regional Aegean extension

The first definitive evidence for regional lithospheric extension is associated with the development of a series of large-scale, bi-vergent low-angle normal faults, including the NCD with top-NE shear, the NPD with top-NNE fabrics, the SCD/WCD and Santorini detachment with top-SW fabrics (Gautier and Brun, 1994; Jolivet et al., 2009a, 2009b, 2010; Ring et al., 2011; Grasemann et al., 2012; Rabailard et al., 2018; Schneider et al., 2018). These low-angle normal faults cross-cut previously ‘frozen in’ metamorphic tectono-stratigraphy and overprint or truncate earlier structures. The NCD crops out on the islands of Andros, Tinos and Mykonos. A geological map of Mykonos, Delos and Rhinia islands is shown in Fig. 13. Jolivet et al. (2010) showed that a series of low-angle detachments, from structurally deepest to highest, include the Tinos detachment active at ca. 21–15 Ma, the Livada detachment active at ca. 14–10 Ma, and the Mykonos detachment, active at ca. 14–9 Ma, which merge upward into one large-scale structure, the NCD that separates Cycladic blueschists in the footwall from the Upper Cycladic nappe in the hanging-wall. These authors proposed that regional extension started in the Oligocene. However, we separate the Oligocene–early Miocene extensional fabrics related to the exhumation of HP and Barrovian facies metamorphic rocks described above, from the Late Miocene–Pliocene detachments (e.g. Livada, Mykonos detachments) related to regional Aegean lithospheric extension. The structurally deeper extensional detachments (e.g. Vari detachment on Syros, Tinos detachment/shear zone, and the Zas and Koronos shear zones on Naxos) are entirely ductile, showing structures associated with exhumation of HP rocks, and kyanite-sillimanite metamorphic rocks in the footwall. The structurally middle detachments (e.g. Livada detachment, Tinos) show early ductile structures with mylonite and ultramylonite shear bands, followed by later brittle structures. The structurally highest and youngest low-angle normal fault in the northern Cyclades islands is the cataclastic-brittle Mykonos detachment with prominent fault gouge along the fault, which separates Late Miocene and younger sediments above from the Upper Cycladic meta-basic rocks, which we interpret as representing the metamorphic sole amphibolites, below (Jolivet et al., 2010; Lecomte et al., 2010). This detachment was initiated at a low angle (<20°), has thick cataclasites along the contact, and has accommodated tens of km of horizontal extension during regional Aegean lithospheric extension (Lecomte et al., 2010).

On Tinos, a series of intrusions bracket the timing of motion on the Tinos detachment/shear zone, (previously interpreted as representing a low-angle normal fault at the base of the NCDS) and brittle normal faulting. U–Pb geochronology on cross-cutting dacite dykes, the Tinos hornblende biotite pluton and garnet bearing leucogranite sills that cut by brittle normal faults suggests that pervasive ductile movement on the Tinos Shear Zone ended by ca. 14.6 Ma, as ductile fabrics are cut by the granites and dacite dykes (Jolivet et al., 2010; Lamont et al., 2020b). A new strain localization, at structurally higher levels around the margins of the granite resulted in steep, brittle normal faults that cut the S-type leucogranite sills (Fig. 12i) and yield ages between ca. 14.8 Ma and 14.2

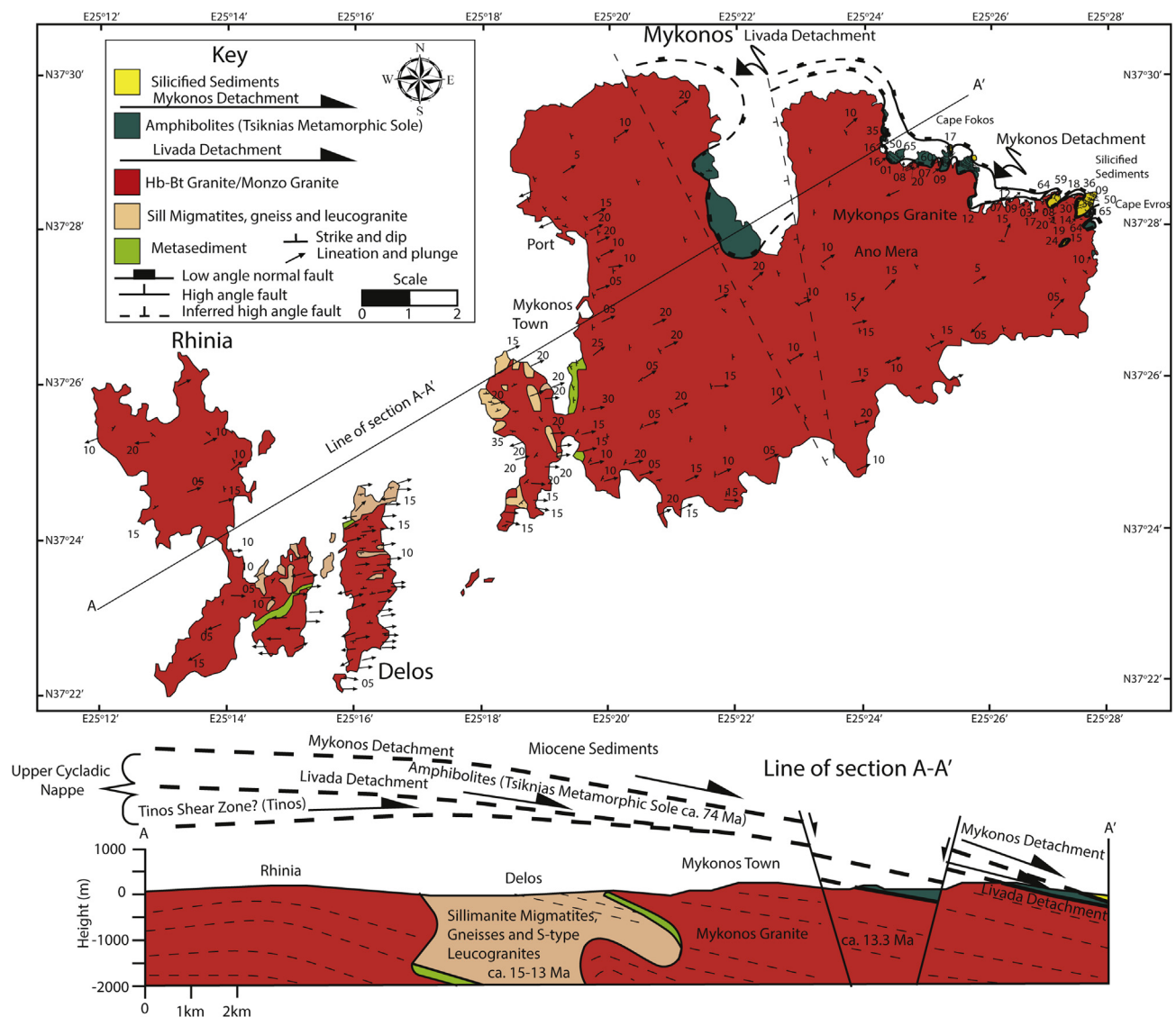


Fig. 13. Geological map of the islands of Rhinia, Delos and Mykonos, after Menant et al. (2013) and our own mapping.

Ma. Brittle deformation associated with regional extension must therefore also be younger than 14.8–14.2 Ma (Lamont et al., 2020a). In contrast, the best age constraint for ductile greenschist facies top-NE shearing on the structure is an Rb–Sr age of ca. 21 Ma (Bröcker and Franz, 1998). These features also suggest that regional scale partial melting and exhumation affected the Cyclades concomitantly with the onset of regional extension at between ca. 15 Ma and 14 Ma.

The Naxos-Paros detachment, a low-angle normal faults have been mapped around the margin of the Naxos metamorphic core complex (Lister et al., 1984; Urai et al., 1990; Buick, 1991; Gautier et al., 1993; Gautier and Brun, 1994; Rey et al., 2001; Kruckenberg et al., 2011; Lamont et al., 2019). The NPD cross-cuts and truncates the contractional structures and top-NE shear fabrics within the interior of the Naxos core complex (Koronos and Zas shear zones) and previously frozen in metamorphic stratigraphy and produces an apparent metamorphic field gradient of up to 700 °C/km. On Naxos, north-south-oriented boudinaged leucogranite dykes and migmatites dated at 15–13 Ma, alongside a U–Pb rutile cooling age of ca. 12.7 Ma (Lamont, 2018), and published ^{40}Ar – ^{39}Ar , fission track, and Rb–Sr ages, indicate that regional extension across Naxos began at ca. 15 Ma (Lamont et al., 2019). Contractional structures reported from Early Miocene sediments in Evia suggest that extension in this area began at ca. 13 Ma (Xypolias et al., 2003). This was

contemporaneous with a two-fold decrease in the convergence rate between Nubia and Eurasia (DeMets et al., 2015) that significantly accelerated cooling rates to 60–90 °C/Myr due to the onset of upper crustal normal faulting that truncates all earlier structures.

Most workers describing regional Aegean extension relate to work along the NE-dipping NCD exposed in many of the Northern Cycladic islands (Jolivet et al., 2009a; 2009b, 2010). Grasemann et al. (2012) described another long (~100 km along strike) low-angle detachment dipping to the SW with top-SSW kinematics, exposed on the islands of Kea, Kythnos and Serifos in the southern Cyclades. Along the South (or West) Cycladic detachment top-south low-angle shearing and normal fault commenced at ~15–13 Ma on Serifos (Grasemann and Petrakakis, 2007; Iglseder et al., 2009), and 13–10 Ma on Sifnos (Ring et al., 2011). A southward dipping detachment with top-south fabrics has recently been mapped on Santorini (Schneider et al., 2018). Interestingly, the hangingwall of this detachment represents unmetamorphosed Triassic limestones possibly related to the Pelagonian Unit on mainland Greece and the footwall represents retrogressed CBU with Ar–Ar cooling ages of 25–19 Ma and zircon fission track ages of 11–8 Ma (Schneider et al., 2018). These dates suggest the structure became active during the Miocene at a similar time to the NCD, NPD and WCD. Thus, the NCD and (S)WCD now show a Late Miocene bivergent extension in the central

Aegean (Grasemann et al., 2012). On the islands of Sifnos, Tinos, Syros and Naxos, earlier, top-NE kinematics have been interpreted as representing the top of a SW-extruding wedge from the subduction zone (Ring and Glodny, 2010; Ring et al., 2011, 2020; Lamont et al., 2019, Lamont et al., 2020b), and not a result of regional horizontal extensional deformation, similar to the interpretation of the structures on Ios (Huet et al., 2009).

9. Coeval I- and S-type granites

The Cyclades records one of the few locations where I- and S-type magmatism intrude in the same geographic location at the same time (Pe-Piper, 2000; Altherr and Siebel, 2002; Koukouvelas and Kokkalas, 2003; Stouraiti et al., 2010; Francalanci and Zellmer, 2019). Available geochronology shows that S-type magmatism (ca. 18–13 Ma; Keay et al., 2001; Beaudoin et al., 2015; Lamont, 2018) slightly pre-dates, or is coeval with, I-type granite crystallization (ca. 15–11 Ma; Brichau et al., 2007; Iglseder et al., 2009; Beaudoin et al., 2015). However, both I- and S-type granites also coincide with regional sillimanite-grade metamorphism and partial melting at the deepest levels of the Cyclades (Keay et al., 2001; Lamont et al., 2019) and are contemporaneous with rapid cooling and exhumation. Jolivet et al. (2015) related the southwestward migration of granites to a slab tear on the Hellenic subduction zone.

Recent isotopic and U–Pb dating suggest that S- and I-type granites on Tinos, Delos and Naxos intruded simultaneously, within the uncertainty of the U–Pb dates. On Tinos this is constrained to between 14.8 Ma and 14.2 Ma, whereas on Naxos intrusion spanned 17–12.2 Ma, and on Delos both types of granite intruded between 13.3 Ma and 12.4 Ma (Lamont, 2018). The unusual coeval nature of I- and S-type magmatism is explained by simultaneous melting of lower crustal Variscan igneous source to form the hornblende-bearing monzogranites, and mid-crustal partial melting of a meta-sedimentary and amphibolite sources to form the garnet-muscovite leucogranites (Altherr and Siebel, 2002; Stouraiti et al., 2010). The limited geographical extent of both granite types suggests that melting was localised and of a crustal origin, as supported by a few isotopic studies (Pe-Piper, 2000; Altherr and Siebel, 2002) and therefore probably not related to subduction-related granites forming above the Hellenic subduction zone.

10. Active extensional tectonics

The active tectonics of the Aegean Sea and Cyclades islands region is controlled by (1) shallow north-dipping subduction of the African plate and attached oceanic lithosphere along the Hellenic subduction zone (Spakman et al., 1988; Jolivet and Brun, 2010), (2) eastward extrusion of Anatolia crust at ~20 mm/yr bounded along the north by the right-lateral North Anatolian strike-slip fault (Armijo et al., 1999), and (3) active stretching and thinning of the crust in the back-arc Aegean Sea region where the Moho is estimated at 25–26 km depth from gravity and seismic data (Cossette et al., 2016). Right-lateral motion along the North Anatolian fault becomes more distributed in the northern Aegean Sea which shows extensive NE–SW aligned normal faults (Kapetanidis and Kassaras, 2019). GPS velocity vectors show NE–SW extension across the Aegean at ~20 mm/yr (Billiris et al., 1991; McClusky et al., 2000). Extension along the Corinth rift system is estimated at a fast rate of 1.5 cm/yr (Armijo et al., 1996). Some authors relate the extension to slab rollback following the decrease of convergence velocity between ~65 Ma and 52 Ma (Jolivet and Brun, 2010). However, England et al. (2016) have shown that the current GPS velocity across the Aegean can be explained by gradients in gravitational potential energy between thick crust under Eurasia and Anatolia, and thin crust at the Hellenic Trench without the requirement of a retreating subduction zone. They argue that tractions applied to the base of the lithosphere from the flowing asthenosphere associated with a retreating slab are insignificant compared to stresses due to gravitational potential energy gradients within the crust. In contradiction to this idea, tomography shows the presence of a long,

steeply-dipping slab beneath the Aegean region that extends down to ca. 1500 km depth (Van Hinsbergen et al., 2005; Jolivet and Brun, 2010), although the resolution of the tomography is inadequate to resolve whether this is just one slab related to the current Hellenic subduction zone, or many slabs related to earlier subduction zones (Dilek and Sandvol, 2009).

HP rocks are also exposed on the island of Crete within the structurally lower Plattenkalk Unit and the overlying Phyllite-Quartzite Unit with HP metamorphic ages of pre- 24 Ma to 20 Ma (Jolivet et al., 1996; Seidel et al., 1982). To explain these much younger high-pressure ages on Crete, we suggest that the thrust front must have migrated southwards during the Oligocene to Miocene in an overall compressional setting (Chatzaras et al., 2006), eventually resulting in the formation of the Mediterranean ridge complex and initiation of the current Hellenic Subduction Zone. It is important to distinguish that in a slab roll-back scenario the entire continental crust between northern Tinos and the current Hellenic trench should have experienced a subduction signature before being accreted to the upper plate. This is clearly not the case as the deepest structural levels and basement of the ACM do not show evidence of high pressures (Van der Maar and Jansen, 1983; Lamont et al., 2019). We propose the geometry of two separate NE-dipping subduction zones, one to the NE of the Cyclades, active during the Late Cretaceous to Eocene, and another (the current Hellenic subduction zone) to the south of the Cyclades active from Oligocene/Late Miocene to present day.

Whereas earthquakes recorded in the western Corinth–Patras rift appear to be active now (Sorel, 2000), in the Cyclades, the low-angle ductile shear zones and normal faults do not appear to be currently active. Steep, active normal faults cut the low-angle normal faults, although many do appear to converge at depth into the low-angle ductile shear zones. There is strong evidence that many of the low-angle normal faults and ductile shear zones are folded around the core complexes (Naxos, Ios), and around the higher structural levels (e.g. Tinos, Sifnos) indicating a possible phase of young, post-low-angle fault, doming. The major low-angle ductile shear zones and normal faults in the Cyclades islands show a large-scale anticline or dome with the axis aligned NW–SE from the Gulf of Evia to the islands of Paros and Naxos (Figs. 2 and 3). Along the NE flank of the dome, the NCD on Andros, Tinos and Mykonos dips at low angles to the NE. Along the SW flank of the dome the S/WCD from offshore Attica to Kea, Kythnos, Serifos, and offshore Sifnos islands, dips at low angles to the SW. Three islands exposing deeper structural levels are the core complexes of Paros, Naxos and Ios, which are located close to the anticline dome axis. The geometry of these structures indicates a large-scale compressional fold with low-angle normal faults slipping off the flanks (Fig. 14). Folding must have occurred during and after low-angle ductile shearing.

On Tinos and Andros islands the major dome axis is orientated NW–SE parallel to the strike of the NCD and active normal faults, with a secondary axis orientated NE–SW. In contrast, on Naxos, Paros and Ios, a tight dome/fold axis is orientated NNE–SSW with a longer wave-length dome axis orientated E–W. This doming/folding is gentle in comparison to the tight, upright isoclinal folding within sillimanite grade migmatites in the core of the Naxos dome suggesting it is un-related to, and post-dates the sillimanite grade metamorphism and deformation. The doming affects the Miocene–Pleistocene continental fluvial sedimentary successions, which are tilted at ca. 15°–30° away from the core complexes (Lamont et al., 2019), indicating that the doming is a very recent feature.

11. Conclusions

The Cyclades experienced a complete cycle of mountain building from the Late-Cretaceous to Middle Miocene, here termed the Aegean Orogeny, prior to regional Aegean extension since ~15 Ma. The mountain belt formed as a result of prolonged crustal shortening between 74 Ma and 15 Ma in a compressional tectonic environment, associated with the closure of an ocean, the Vardar ocean, to the NE of the Cyclades in the

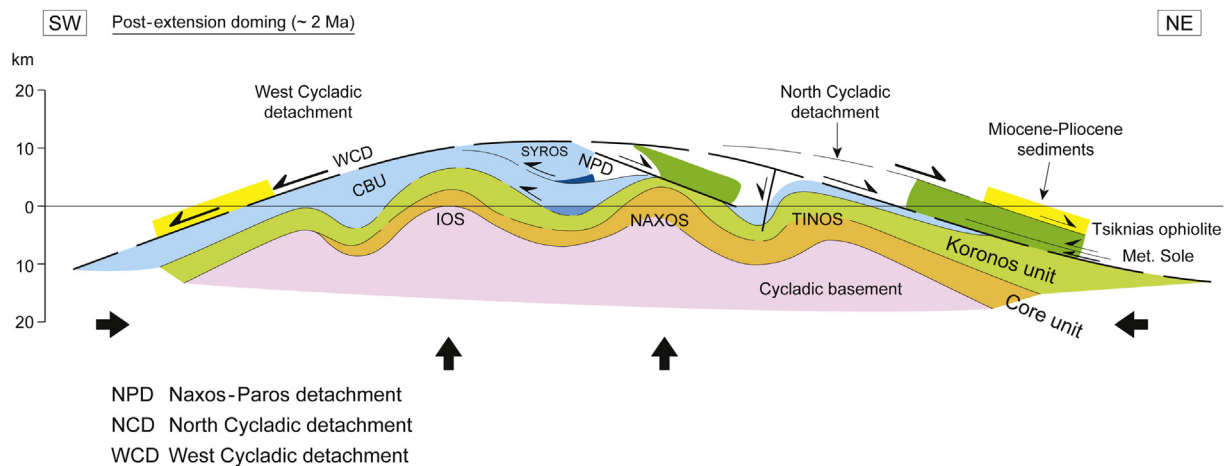


Fig. 14. Schematic section across the Cyclades islands showing NW-SE aligned anticlinal fold with low-angle normal faults verging NE along the North Cycladic Detachment, and SW along the West Cycladic Detachment, indicating large-scale slip off the flanks of the Cycladic dome.

present-day co-ordinates. The Aegean orogeny shows all stages of a classic Wilson cycle from ophiolite obduction, subduction of the continental margin, through collision and crustal thickening, to post-orogenic collapse and extension. Our main conclusions can be summarised, with reference to the tectonic stratigraphic columns (Fig. 4), the tectonic model (Fig. 8), and the time chart (Fig. 15), as follows:

- (1) The early part of the Aegean orogeny involved SW-directed obduction of the Tsiknias Ophiolite onto the previously passive continental margin of the Adria plate. Obduction is recorded in the amphibolite facies metamorphic sole cropping out immediately beneath the ophiolite mantle sequence harzburgites and dunite. The ophiolite was formed in the Jurassic with U-Pb zircon ages from a plagiogranite of 161.9 ± 2.8 Ma and a gabbro at 144.4 ± 5.6 Ma, whereas the metamorphic sole amphibolites were formed much later at 74.0 ± 5.6 Ma (Lamont et al., 2020a). We interpret the metamorphic sole age as timing the initiation of subduction and obduction of a slice of older Jurassic oceanic crust and upper mantle. The Tsiknias ophiolite and metamorphic sole has been cut by later, low-angle normal faults above (Livada detachment) and below (Tinos detachment; Jolivet et al., 2010).
- (2) Oceanic crustal sequence gabbros, basalts and manganiferous cherts were subducted to the NE and reached peak eclogite facies depths of around 80–90 km. Lawsonite-bearing blueschists and eclogites on Tinos have P-T conditions of 26–22 kbar and 570–500 °C (Lamont et al., 2020b). Exhumation of these eclogites and blueschists cannot be explained by regional extension and require a subduction zone setting. These rocks were exhumed back along the subduction channel recording widespread exhumation showing top-NE, base-SW ‘extensional’ fabrics, coeval with underthrusting of rocks that did not reach as high-pressure, in a wholly compressional tectonic setting (Xypolias et al., 2003, 2012; Chatzaras et al., 2006; Xypolias and Kokkalas, 2006; Huet et al., 2009; Ring et al., 2010, 2020; Xypolias and Alsop, 2014; Lamont et al., 2020b). Eclogites and structurally overlying blueschists show ubiquitous tight-isoclinal folding and localised top-SW, base-NE thrust fabrics, with higher pressure rocks thrust over lower pressure rocks, indicating they were exhumed in an overall compressional stress environment. Most of the ‘extensional’ S-C fabrics and kinematic indicators in the eclogites and the Cycladic blueschists from Syros, Tinos, and Sifnos, were formed by SW-directed expulsion from the subduction channel and extrusion beneath a passive roof fault, and not by regional Aegean extension.
- (3) Tight – isoclinal folding, horizontal constriction, vertical stretching in regional kyanite-sillimanite grade rocks in the Naxos metamorphic core complex clearly record partial melting and kyanite-sillimanite grade metamorphism in an overall compressional environment with crustal shortening and thickening following continent-continent collision between Eurasia and the Cyclades/Adria (Lamont et al., 2019; Searle and Lamont, 2019). Pressures recorded in these rocks (~10 kbar) are far greater than can be accounted for by regional extension and isostatic uplift alone. ‘Extensional’ fabrics within the interior of the Naxos metamorphic core complex were related to SW-extrusion of footwall rocks beneath a passive roof fault or low-angle extensional detachment (e.g. Koronos and Zas Shear Zones on Naxos).
- (4) One major, large-scale, low-angle ductile shear zone with associated brittle normal faults, has been mapped along the NE-dipping North Cycladic Detachment (NCD) exposed along the margins of Andros, Tinos, Mykonos, and Ikaria and showing consistent extensional top-NE kinematic indicators (e.g. Jolivet et al., 2010; Lecomte et al., 2010; Menant et al., 2013). A second large-scale ductile shear zone and normal fault has been mapped along the SW-dipping West Cycladic Detachment system (WCD) which crops out for at least 100 km along strike along the margins of the islands of Kea, Kythnos, Sifnos (Grasemann et al., 2012; Coleman et al., 2019). Both these extensional shear zones were active from ~15 Ma and do indicate large-scale upper crustal extension (Jolivet et al., 2009a, 2009b, 2010; Jolivet and Brun, 2010; Grasemann et al., 2012; Menant et al., 2016).
- (5) The NCD and the WCD formed along the flanks of a major NW-SE oriented gentle anticline with a wavelength of ca. 100 km. These large-scale shear zones record regional slip away from the central axis, possibly recording upper crustal extensional slip off the flanks of a 100 km wavelength growing anticline. On many islands these regional extensional detachments have been folded by subsequent doming (Naxos, Ios, Paros, Sifnos) recording a Quaternary period of W-E shortening following regional Aegean extension. The cause of this shortening remains speculative. It may be a result of the onset of dextral slip along the North Anatolian Fault system at ca. 11 Ma and westward motion of Anatolia (Menant et al., 2013), although the North Anatolian faults do not extend south of the northern Cycladic islands and the NCD backstop (Jolivet et al., 2010).
- (6) The youngest and active phase in the Cyclades islands is another renewed period of lithospheric extension as recorded in active steep normal faults and extensional earthquakes in the Northern Aegean region to the north and NE of the Cyclades islands, and the

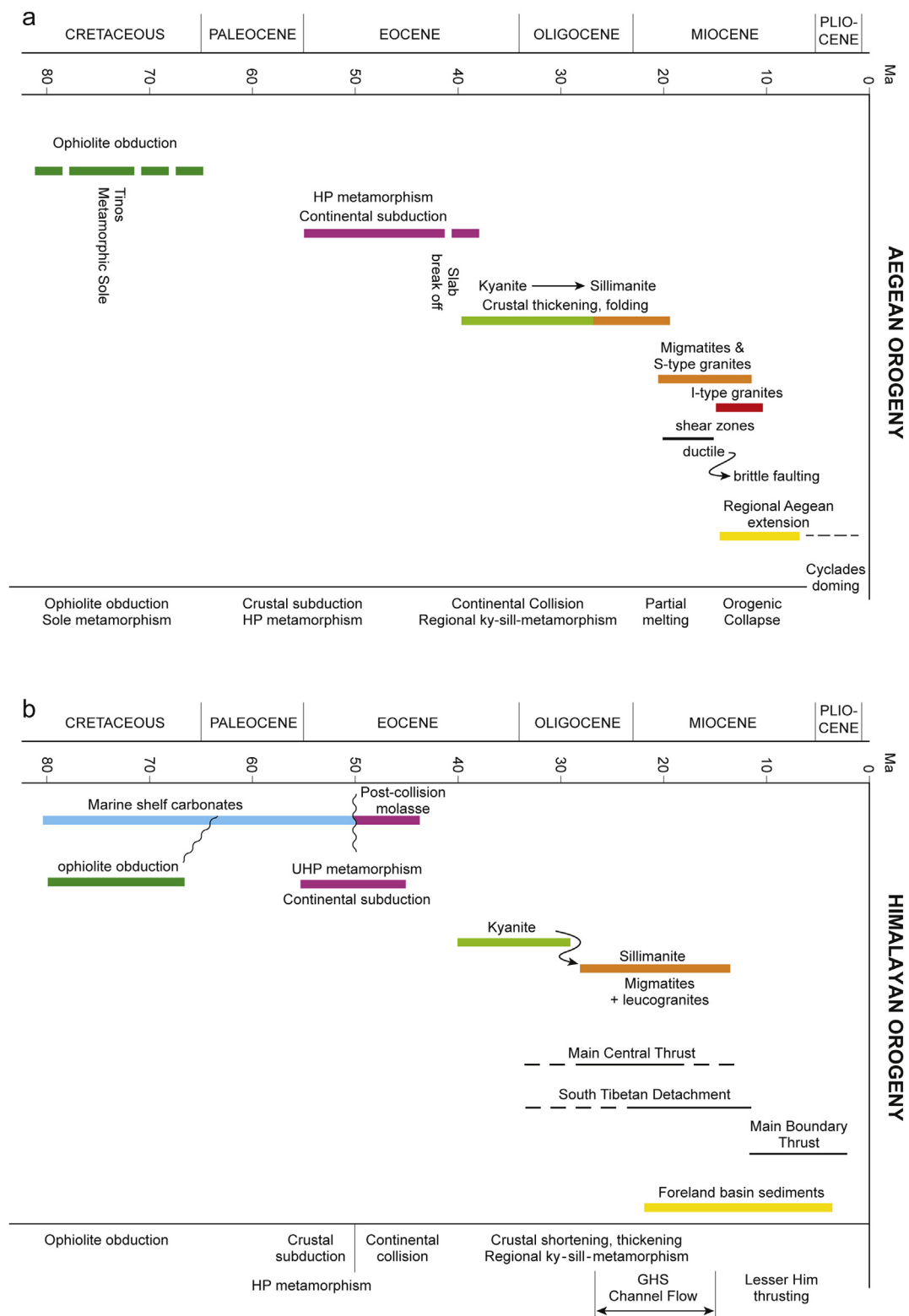


Fig. 15. Time charts showing tectonic evolution for (a) the Aegean orogeny and (b) Himalayan orogeny. See text for all sources of age data. Note the similarities in timings for each stage of ophiolite obduction (green), followed by crustal subduction and HP metamorphism (pink), continental collision and regional Barrovian (kyanite [light green], and sillimanite [orange] grade) metamorphism. Time span of regional Aegean extension (yellow) is not matched in the Himalaya which has not yet undergone orogenic collapse. The yellow bar is the timing of foreland basin deposition in the Siwalik basin south of the Himalayan front. See text for sources of age data for the Aegean, and the review of Himalayan ages in [Searle \(2015\)](#).

mainland region in the Peloponnese – Corinth area, and also along the volcanic arc. Earthquakes in the Corinth-Patras rift suggest nucleation along a low-angle (20°) fault at depth (Reitbroch et al., 1996; Sorel, 2000). High-angle normal faults merge at depth into this low-angle detachment. Very few earthquakes occur within the Cyclades. The 1956 Amorgos Mw 7.5 earthquake was related to extension along the Santorini volcanic arc, and not to tectonics of the Cyclades islands.

- (7) Time constraints of each stage of the Wilson cycle constrained by geochronology matches very closely with time scales of ophiolite obduction in Oman, crustal subduction and (U)HP metamorphism, crustal thickening and regional Barrovian (kyanite, sillimanite) metamorphism and partial melting in the Himalayan orogeny (Fig. 15). The Aegean orogeny has close similarities to the Himalaya in many respects, but has, in addition, undergone post-orogenic collapse, a phase which has not yet affected the Himalaya.
- (8) Continuous slab rollback and regional extension since the Eocene cannot explain the metamorphism and structures within continental crustal rocks in the Cyclades. It is more likely that the geodynamic evolution of the Aegean Sea – Cyclades islands involved (a) a Late Cretaceous–Eocene NE-dipping subduction zone responsible for ophiolite obduction and HP metamorphism of the Cycladic/Adriatic continental margin, rooted to the suture zone NE of the Cyclades in present day co-ordinates, and (b) a younger NE-dipping subduction zone to the south of the Cyclades, active from the early Miocene and associated with Crete blueschists, that continued until the present day as the Hellenic Subduction Zone.

Declaration of competing interest

The authors declare that they have no known competing financial interests or personal relationships that could have appeared to influence the work reported in this paper.

Acknowledgments

We acknowledge with gratitude Natural Environment Research Council grant NE/L0021612/1 and NERC Isotope Geoscience Laboratory grant IP-1597-1115 for funding. We are very grateful to Sotirios Kokkalas, Paris Xypolias, Chris Ballhaus, Laurent Jolivet, Valentin, Laurent, Michael Bröcker, Nick Roberts, Tony Watts and Philip England for discussions. We thank Chris Ballhaus for introducing us to the geology of Syros island, Paris Xypolias and Bernhard Grasemann for detailed comments on an earlier draft of the manuscript, and M. Santosh and Richard Palin for editorial handling.

References

Altherr, R., Siebel, W., 2002. I-type plutonism in a continental back-arc setting: Miocene granitoids and monzonites from the central Aegean Sea, Greece. *Contrib. Mineral. Petrol.* 143, 397–415. <https://doi.org/10.1007/s00410-002-0352-y>.

Aravadinou, E., Xypolias, P., 2017. Evolution of a passive crustal-scale detachment (Syros, Aegean region): insights from a structural and petrofabric analyses in the hanging-wall. *J. Struct. Geol.* 103, 57–74.

Armijo, R., Meyer, B., King, G.C.P., Rigo, A., Papanastassiou, D., 1996. Quaternary evolution of the Corinth rift and its implications for the late Cenozoic evolution of the Aegean. *Geophys. J. Int.* 126, 11–53.

Armijo, R., Meyer, B., Hubert, A., Barka, A., 1999. Westward propagation of the North Anatolian fault into the northern Aegean: timing and kinematics. *Geology* 27 (3), 267–270.

Beaudoin, A., Augier, R., Laurent, V., Jolivet, L., Lahfid, A., Bossé, V., Arbaret, L., Rabillard, A., Menant, A., 2015. The Ikaria high-temperature metamorphic core complex (Cyclades, Greece): geometry, kinematics and thermal structure. *J. Geodyn.* 92, 18–41. <https://doi.org/10.1016/j.jog.2015.09.004>.

Baziotis, I., 2020. Exhumation of Attica high-pressure rocks in a subduction channel: New metamorphic PT constraints from Attica, NW Cyclades, Greece. *Lithos*. <https://doi.org/10.1016/j.lithos.2019.105266>.

Billiris, H., Paradissis, D., Veis, G., England, P., Featherstone, W., Parsons, B., Cross, P., Rands, P., Rayson, M., Sellers, P., Ashkenazi, V., Davison, M., Jackson, J.,

Ambraseys, N., 1991. Geodetic determinations of tectonic deformation in central Greece from 1900 to 1988. *Nature* 350, 124–129.

Brichau, S., Ring, U., Carter, A., Monie, P., Bolhar, R., Stockli, D., Brunel, M., 2007. Extensional faulting on Tinos island, Greece: how many detachments? *Tectonics* 26, TC4009. <https://doi.org/10.1029/2006TC001969>.

Bröcker, M., Kreuzer, H., Matthews, A., Okrusch, M., 1993. ⁴⁰Ar/³⁹Ar and oxygen isotope studies of polymetamorphism from Tinos Island, Cycladic blueschist belt, Greece. *J. Metamorph. Geol.* 11, 223–240. <https://doi.org/10.1111/j.1525-1314.1993.tb00144.x>.

Bröcker, M., Enders, M., 1999. U-Pb zircon geochronology of unusual eclogite-facies rocks from Syros and Tinos (Cyclades, Greece). *Geol. Mag.* 136, 111–118.

Bröcker, M., Enders, M., 2001. Unusual bulk-rock composition in eclogite-facies rocks from Syros and Tinos (Cyclades, Greece): implications for U-Pb zircon geochronology. *Chem. Geol.* 175, 581–603.

Bröcker, M., Löwen, K., Rodionov, N., 2014. Unravelling protolith ages of meta-gabbros from Samos and the Attic-Cycladic crystalline belt, Greece: results of a U-Pb zircon and Sm-Nd whole rock study. *Lithos* 198, 234–248.

Buick, I.S., 1991. The late Alpine evolution of an extensional shear zone, Naxos, Greece. *J. Geol. Soc.* 148 (1), 93–103.

Buick, I.S., Holland, T.J.B., 1989. The P-T-t path associated with crustal extension, Naxos Cyclades, Greece. In: Daly, J.S., Cliff, R.A., Yardley, B.W.D. (Eds.), *Evolution of Metamorphic Belts*. Geological Society, London, Special Publication, pp. 365–369.

Bulle, F., Bröcker, M., Gärtner, C., Keasling, A., 2010. Geochemistry and geochronology of HP mélanges from Tinos and Andros, cycladic blueschist belt, Greece. *Lithos* 117, 61–81. <https://doi.org/10.1016/j.lithos.2010.02.004>.

Chatzaras, V., Xypolias, P., Doutsos, T., 2006. Exhumation of high-pressure rocks under continuous compression: a working hypothesis for the southern Hellenides (central Crete, Greece). *Geol. Mag.* 143 (6), 859–876.

Coleman, M., Dubosq, R., Schneider, D.A., Grasemann, B., Soukis, K., 2019. Along-strike consistency of an extensional detachment system, West Cyclades, Greece. *Terra Nova* 31, 220–233.

Cossette, É., Audet, P., Schneider, D., Grasemann, B., 2016. Structure and anisotropy of the crust in the Cyclades, Greece, using receiver functions constrained by in situ rock textural data. *J. Geophys. Res. Solid Earth* 121, 2661–2678. <https://doi.org/10.1002/2015JB012460>.

DeMets, C., Iaffaldano, G., Merkouriev, S., 2015. High-resolution Neogene and Quaternary estimates of Nubia-Eurasia-north America plate motion. *Geophys. J. Int.* 203, 416–427. <https://doi.org/10.1093/gji/ggv277>.

Dilek, Y., Sandvol, E., 2009. Seismic structure, crustal architecture and tectonic evolution of the Anatolian–African Plate Boundary and the Cenozoic Orogenic Belts in the Eastern Mediterranean Region. In: Murphy, J.B., Keppie, J.D., Hynes, A.J. (Eds.), *Ancient Orogens and Modern Analogues*, vol. 327. Geological Society, London, Special Publications, pp. 127–160.

Dragovic, B., Samanta, L.M., Baxter, E.F., Selverstone, J., 2012. Using garnet to constrain the duration and rate of water releasing metamorphic reactions during subduction: an example from Sifnos, Greece. *Chem. Geol.* 314, 9–22.

England, P., Holland, T.J.B., 1979. Archimedes and the Tauern eclogites: the role of buoyancy in the preservation of exotic eclogite blocks. *Earth Planet. Sci. Lett.* 44, 287–294.

England, P.C., Houseman, G., Nocquet, J.M., 2016. Constraints from GPS measurements on the dynamics of deformation in Anatolia and the Aegean. *J. Geophys. Res. Solid Earth* 121, 8888–8916. <https://doi.org/10.1002/2016JB013382>.

Floyd, M.A., Billiris, H., Paradissis, D., Veis, G., Avallone, A., Briole, P., McClusky, S., Nocquet, J.-M., Palamartchouk, K., Parsons, B., England, P.C., 2010. A new velocity field for Greece: implications for the kinematics and dynamics of the Aegean. *J. Geophys. Res. Solid Earth* 115, B10403. <https://doi.org/10.1029/2009JB007040>.

Francalanci, L., Zellmer, G.F., 2019. Magma genesis at the South Aegean volcanic arc. *Elements* 15 (3), 165–170. <https://doi.org/10.2138/gselements.15.3.165>.

Gautier, P., Brun, J.-P., 1994. Crustal-scale geometry and kinematics of late orogenic extension in the central Aegean (Cyclades and Evvia island). *Tectonophysics* 238, 399–424.

Gautier, P., Brun, J.-P., Jolivet, L., 1993. Structure and kinematics of upper crustal extensional detachment on Naxos and Paros (Cyclades islands, Greece). *Tectonics* 12, 1180–1194. <https://doi.org/10.1029/93TC01131>.

Gerogiannis, N., Xypolias, P., Chatzaras, V., Aravadinou, E., Papapavlou, K., 2019. Deformation within the Cycladic subduction – exhumation channel: new insights from the enigmatic Makrotantalo nappe (Andros, Aegean). *Int. J. Earth Sci.* 108, 817–843.

Grasemann, B., Petrakakis, K., 2007. Evolution of the Serifos metamorphic core complex. In: Lister, G., Forster, M., Ring, U. (Eds.), *Inside the Aegean Metamorphic Core Complexes*. Journal of the Virtual Explorer, vol. 27, pp. 1–18. <https://doi.org/10.3809/jvirtex.2007.00170>.

Grasemann, B., Schneider, D.A., Stockli, D., Iglseder, C., 2012. Miocene divergent crustal extension in the Aegean: evidence from the western Cyclades (Greece). *Lithosphere* 4 (1), 23–39. <https://doi.org/10.1130/L164.1>.

Grasemann, B., Huet, B., Schneider, D.A., Rice, H.N., Lemonnier, N., Tschegg, C., 2017. Miocene postorogenic extension of the Eocene synorogenic imbricated Hellenic subduction channel: new constraints from Milos (Cyclades, Greece). *Geol. Soc. Am. Bull.* 130, 238–262. <https://doi.org/10.1130/B31731.1>.

Hacker, B.R., Gerya, T.V., 2013. Paradigms new and old for ultrahigh-pressure tectonism. *Tectonophysics* 603, 79–88.

Hanmer, S., Passchier, C., 1991. Shear-sense indicators: a review. *Geol. Survey Canada* 90–17, 72p.

Hinsken, T., Bröcker, M., Berndt, J., Gärtner, C., 2016. Maximum sedimentation ages and provenance of metasedimentary rocks from Tinos Island, Cycladic blueschist belt, Greece. *Int. J. Earth Sci.* 105, 1923. <https://doi.org/10.1007/s00531-015-1258-z>.

- Huet, B., Labrousse, L., Jolivet, L., 2009. Thrust or detachment? Exhumation processes in the Aegean: insight from a field study on Ios (Cyclades, Greece). *Tectonics* 28, TC3007. <https://doi.org/10.1029/2008TC002397>.
- Iglseder, C., Grasmann, B., Schneider, D.A., Petrakakis, K., Miller, C., Klötzli, U.S., Thöni, M., Zámolyi, A., Rambousek, C., 2009. I- and S-type plutonism on Serifos (W-Cyclades, Greece). *Tectonophysics* 473 (1–2), 69–83. <https://doi.org/10.1016/j.tecto.2008.1009.1021>.
- Jolivet, L., 2001. A comparison of geodetic and finite strain in the Aegean: geodynamic implications. *Earth Planet Sci. Lett.* 187, 94–104.
- Jolivet, L., Brun, J.-P., 2010. Cenozoic geodynamic evolution of the Aegean. *Int. J. Earth Sci.* 99, 109–138. <https://doi.org/10.1007/s00531-008-0366-4>.
- Jolivet, L., Goffé, B., Monié, P., Truffert-Luxey, C., Patriat, M., Bonneau, M., 1996. Miocene detachment in Crete and exhumation P-T-t paths of high-pressure metamorphic rocks. *Tectonics* 15 (6), 1129–1153.
- Jolivet, L., Labrousse, L., Agard, P., Lacombe, O., Bailly, V., Lecomte, E., Mouthereau, F., Mehl, C., 2009a. Rifting and shallow-dipping detachments, clues from the Corinth Rift and the Aegean. *Tectonophysics* 483 (3–4), 287–304. <https://doi.org/10.1016/j.tecto.2009.11.001>.
- Jolivet, L., Lecomte, E., Huet, B., Denele, Y., Lacombe, O., Labrousse, L., Pourhiet, L., Mehl, C., 2010. The North Cycladic Detachment System. *Earth Planet Sci. Lett.* 289, 87–104. <https://doi.org/10.1016/j.epsl.2009.10.032>.
- Jolivet, L., Faccenna, C., Piromallo, C., 2009b. From mantle to crust: stretching the Mediterranean. *Earth Planet Sci. Lett.* 285, 198–209. <https://doi.org/10.1016/j.epsl.2009.06.017>.
- Jolivet, L., Menant, A., Sternai, P., Rabillard, A., Arbaret, L., Augier, R., Laurent, V., Beaudoin, A., Grasmann, B., Huet, B., Labrousse, L., LePourhiet, L., 2015. The geological signature of a slab tear below the Aegean. *Tectonophysics* 659, 166–182.
- Kapetanidis, V., Kassaras, I., 2019. Contemporary crustal stress of the Greek region deduced from earthquake focal mechanisms. *J. Geodyn.* 123, 55–82.
- Keay, S., Lister, G., Buick, I., 2001. The timing of partial melting, Barrovian metamorphism and granite intrusion in the Naxos metamorphic core complex, Cyclades, Aegean Sea, Greece. *Tectonophysics* 342, 275–312.
- Keiter, M., Ballhaus, C., Tomaschek, F., 2011. A new geological map of the island of Syros (Aegean Sea, Greece): implications for lithostratigraphy and structural history of the cycladic blueschist unit. *Geol. Soc. Am. Spec. Pap.* 481, 1–43.
- Keiter, M., Piepjohn, K., Balhaus, C., Lagos, M., Bode, M., 2004. Structural development of high-pressure metamorphic rocks on Syros island (Cyclades, Greece). *J. Struct. Geol.* 26, 1433–1445.
- Kokkalas, S., Doutsos, T., 2001. Strain-dependent stress field and plate motions in the southeast Aegean region. *J. Geodyn.* 32, 311–332.
- Koukouvelas, I.K., Kokkalas, S., 2003. Emplacement of the Miocene west Naxos pluton (Aegean Sea, Greece): a structural study. *Geol. Mag.* 140, 45–61. <https://doi.org/10.1017/S0016756802007094>.
- Kruckenberger, S.C., Vanderhaeghe, O., Ferré, E.C., Teyssier, C., Whitney, D.L., 2011. Flow of partially molten crust and the internal dynamics of a migmatite dome, Naxos, Greece. *Tectonics* 30, TC3001. <https://doi.org/10.1029/2010TC002751>.
- Lagos, M., Scherer, E.E., Tomaschek, F., Münker, C., Keiter, M., Berndt, J., Ballhaus, C., 2007. High-precision Lu-Hf geochronology of Eocene eclogite-facies rocks from Syros, Cyclades, Greece. *Chem. Geol.* 243, 16–35.
- Lamont, T.N., 2018. Unravelling the Structural, Metamorphic, and Strain History of the Aegean Orogeny, Southern Greece with a Combined Structural, Petrological and Geochronological Approach. Unpublished D.Phil thesis. University of Oxford, UK.
- Lamont, T.N., Searle, M.P., Gopon, P., Roberts, N.M.W., Wade, J., Palin, R.M., Waters, D.J., 2020b. The Cycladic blueschist unit on Tinos, Greece: cold NE subduction and SW-directed extrusion of the Cycladic continental margin under the Tsiknias ophiolite. *Tectonics*. <https://doi.org/10.1029/2019TC005890>. In press.
- Lamont, T.N., Searle, M.P., Roberts, N.M.W., Waters, D.J., Palin, R.M., Smye, A.J., Dyck, B., Gopon, P., Weller, O.M., St-Onge, M., 2019. Compressional origin to the Naxos metamorphic core complex, Greece: structure, petrography and thermobarometry. *Geol. Soc. Am. Bull.* 132, 149–197. <https://doi.org/10.1130/B31978.1>.
- Lamont, T.N., Roberts, N.M.W., Searle, M.P., Gopon, P., Waters, D.J., Millar, I., 2020a. The age, origin and emplacement of the Tsiknias ophiolite, Tinos, Greece. *Tectonics* 39, e2019TC005677. <https://doi.org/10.1029/2019TC005677>.
- Laurent, V., Jolivet, L., Roche, V., Augier, R., Scaillet, S., Cardello, G.L., 2016a. Strain localization in a fossilized subduction channel: insights from the cycladic blueschist unit, (Syros, Greece). *Tectonophysics* 672, 150–169.
- Laurent, V., Huet, B., Labrousse, L., Jolivet, L., Monié, P., Augier, R., 2016b. Extraneous origin in high-pressure metamorphic rocks: distribution, origin and transport in the Cycladic Blueschist Unit (Greece). *Lithos* 272–3, 315–335.
- Laurent, V., Lanari, P., Nair, I., Augier, R., Lahfid, A., Jolivet, L., 2018. Exhumation of eclogite and blueschist (Cyclades, Greece): pressure-temperature evolution determined by thermobarometry and garnet equilibrium modelling. *J. Metamorph. Geol.* 36, 769–798.
- Law, R.D., Searle, M.P., Godin, L., 2006. Channel Flow, Ductile Extrusion and Exhumation in Continental Collision Zones. Geological Society, London, Special Publication, p. 620.
- Lecomte, E., Jolivet, L., Lacombe, O., Denele, Y., Labrousse, L., Le Pourhiet, L., 2010. Geometry and kinematics of Mykonos detachment, Cyclades, Greece: evidence for slip at shallow dip. *Tectonics* 29, TC5012. <https://doi.org/10.1029/2009tc002564>.
- Lister, G.S., Banga, G., Feenstra, A., 1984. Metamorphic core complexes of cordilleran type in the Cyclades, Aegean Sea, Greece. *Geology* 12, 221–225.
- Martin, L., Duchene, S., Deloule, E., Vanderhaeghe, O., 2006. The isotopic composition of zircon and garnet: a record of the metamorphic history of Naxos, Greece. *Lithos* 87, 174–192.
- McClusky, S., Balassanian, S., Barka, A., Demir, C., Veis, G., 2000. Global Positioning System constraints on plate kinematics and dynamics in the eastern Mediterranean and Caucasus. *J. Geophys. Res.* 105 (B3), 5695–5720.
- McKenzie, D., Jackson, J., 1983. The relationship between strain rate, crustal thickening, palaeomagnetism, finite strain and fault movements within a deforming zone. *Earth Planet Sci. Lett.* 65, 182–202.
- Means, W., 1989. Stretching faults. *Geology* 17, 893–896.
- Menant, A., Jolivet, L., Augier, R., Skarpeis, N., 2013. The North Cycladic Detachment System and associated mineralization, Mykonos, Greece: insights on the evolution of the Aegean domain. *Tectonics* 32, 433–452. <https://doi.org/10.1002/tect.20037>.
- Menant, A., Jolivet, L., Vrielynnck, B., 2016. Kinematic reconstructions and magmatic evolution illuminating crustal and mantle dynamics of the eastern Mediterranean region since late Cretaceous. *Tectonophysics* 675, 103–140.
- Nocquet, J.-M., 2012. Present-day kinematics of the Mediterranean: a comprehensive overview of GPS results. *Tectonophysics* 579, 220–242.
- Papazachos, C.B., 2019. Deep structure and active tectonics of the south aegean volcanic arc. *Elements* 15 (3), 153–158. <https://doi.org/10.2138/gselements.15/3/153>.
- Passchier, C.W., Trouw, R.A.J., 1996. *Micro-tectonics*. Springer-Verlag, Heidelberg, p. 289.
- Peillod, A., Ring, U., Glodny, J., Skelton, A., 2017. An Eocene/Oligocene blueschist-/greenschist PT loop from Cycladic Blueschist unit on Naxos Island, Greece: deformation related re-equilibrium vs thermal relaxation. *J. Metamorph. Geol.* 35, 805–830. <https://doi.org/10.1111/jmg.12256>.
- Pe-Piper, G., 2000. Origin of S-type granites coeval with I-type granites in the Hellenic subduction system, Miocene of Naxos, Greece. *Eur. J. Mineral* 12 (4), 859–875.
- Philippon, M., Brun, J.-P., Gueydan, F., 2011. Tectonics of the Syros blueschists (Cyclades, Greece): from subduction to aegean extension. *Tectonics* 30, TC4001. <https://doi.org/10.1029/2010TC002810>.
- Philippon, M., Brun, J.-P., Gueydan, F., 2012. Deciphering subduction from exhumation in the segmented Cycladic Blueschist Unit (Central Aegean, Greece). *Tectonophysics* 524, 116–134. <https://doi.org/10.1016/j.tecto.2011.12.025>.
- Platt, J.P., Vissers, R.L.M., 1980. Extensional structures in anisotropic rocks. *J. Struct. Geol.* 2, 397–410.
- Rabailard, A., Jolivet, L., Arbaraet, L., Bessiere, E., Laurent, V., Menant, A., Augier, R., Beaudoin, A., 2018. Synextensional granitoids and detachment systems within cycladic metamorphic core complexes (Aegean Sea, Greece): toward a regional tectonomagmatic model. *Tectonics* 37, 2328–2362. <https://doi.org/10.1029/2017TC004697>.
- Reilinger, R., McClusky, S., Vernant, P., Lawrence, S., Ergintav, S., Cakmak, R., Ozener, H., Kadirov, F., Guliev, I., Stepanyan, R., Nadariya, M., Hahubia, G., Mahmoud, S., Sakr, K., ArRajehi, A., Paradissis, D., Al-Aydrus, A., Prilepin, M., Guseva, T., Evren, E., Dmitrova, A., Filikov, S.V., Gomez, F., Al-Ghazzi, R., Karam, G., 2006. GPS constraints on continental deformation in the Africa-Arabia-Eurasia continental collision zone and implications for the dynamics of plate interactions. *J. Geophys. Res.* 111, B05411. <https://doi.org/10.1029/2005JB004051>.
- Reitbroch, A., Tiberi, C., Scherbaum, F., Lyon-Caen, H., 1996. Seismic slip along a low-angle normal fault in the Gulf of Corinth: evidence from high-resolution cluster analysis of micro-earthquakes. *Geophys. Res. Lett.* 23, 1817–1820.
- Rey, P., Vanderhaeghe, O., Teyssier, C., 2001. Gravitational collapse of the continental crust: definition, regime and modes. *Tectonophysics* 342, 435–449. [https://doi.org/10.1016/S0040-1951\(01\)00174-3](https://doi.org/10.1016/S0040-1951(01)00174-3).
- Rey, P., Teyssier, C., Kruckenberger, S., Whitney, D.L., 2011. Viscous collision in channel explains double domes in metamorphic core complexes. *Geology* 39 (4), 387–390. <https://doi.org/10.1130/G31587.1>.
- Rey, P.F., Mondy, L., Duclaux, G., Teyssier, C., Whitney, D.L., Bocher, M., Prigent, C., 2017. The origin of contractional structures in extensional gneiss domes. *Geology* 45, 263–266.
- Ring, U., Glodny, J., 2010. No need for lithospheric extension for exhuming (U)HP rocks by normal faulting. *J. Geol. Soc., London* 167, 225–228.
- Ring, U., Glodny, J., Will, T., Thomson, S., 2007. An Oligocene extrusion wedge of blueschist facies nappes on Evia, Aegean Sea, Greece: implications for the early exhumation of HP rocks. *J. Geol. Soc., London* 164, 637–652.
- Ring, U., Glodny, J., Will, T., Thomson, S., 2010. The Hellenic subduction system: high-pressure metamorphism, exhumation, normal faulting and large-scale extension. *Annu. Rev. Earth Planet Sci.* 38, 45–76. <https://doi.org/10.1146/annurev.earth.050708.170910>.
- Ring, U., Glodny, J., Will, T., Thomson, S., 2011. Normal faulting on Sifnos and the south cycladic detachment system, Aegean Sea, Greece. *J. Geol. Soc., London* 168, 751–768.
- Ring, U., Pantazides, H., Glodny, J., Skelton, A., 2020. Forced return flow deep in the subduction channel, Syros, Greece. *Tectonics* 39, e2019TC005768. <https://doi.org/10.1029/2019TC005768>.
- Roche, V., Laurent, V., Cardello, G.L., Jolivet, L., Scaillet, S., 2016. Anatomy of the Cycladic Blueschist Unit on Sifnos Island (Cyclades, Greece). *J. Geodyn.* 97, 62–87.
- Schneider, D.A., Grasmann, B., Lion, A., Soukis, K., Draganits, E., 2018. Geodynamic significance of the Santorini detachment system (Cyclades, Greece). *Terra Nova* 30, 414–422.
- Searle, M.P., 2010. Low-angle normal faults in the compressional Himalayan orogen: evidence from the Annapurna-Dhaulagiri Himalaya, Nepal. *Geosphere* 6, 296–315. <https://doi.org/10.1130/GES00549.1>.
- Searle, M.P., 2015. Mountain Building, Tectonic Evolution, Rheology, and Crustal Flow in the Himalaya, Karakoram, and Tibet. In: Schubert, G. (Ed.), *Treatise on Geophysics* (Second Edition), vol. 6. Elsevier, pp. 469–511.
- Searle, M.P., Lamont, T.N., 2019. Compressional metamorphic core complexes, low-angle normal faults and extensional fabrics in compressional tectonic settings. *Geol. Mag.* 118. <https://doi.org/10.1017/S0016756819000207>.

- Searle, M.P., Law, R.D., Jessup, M.J., 2006. Crustal structure, restoration and evolution of the Greater Himalaya in Nepal-South Tibet: implications for channel flow and ductile extrusion of the middle crust. *Geol. Soc. London, Special Publication* 268, 355–378.
- Searle, M.P., Waters, D.J., Martin, H.N., Rex, D.C., 1994. Structure and metamorphism of blueschist-eclogite facies rocks from the northeastern Oman Mountains. *J. Geol. Soc., London* 151, 555–576.
- Seidel, E., Kreuzer, H., Harre, W., 1982. A late Oligocene/early Miocene high pressure belt in the external hellenides. *Geol. J. E23*, 165–206.
- Shaw, B., Jackson, J., 2010. Earthquake mechanisms and active tectonics of the Hellenic subduction zone. *Geophys. J. Int.* 181 (2), 966–984. <https://doi.org/10.1111/j.1365-246x.2010.04551.x>.
- Sorel, D., 2000. A Pleistocene and still-active detachment fault and the origin of the Corinth-Patras rift, Greece. *Geology* 28, 83–86.
- Soukis, K., Stockli, D.F., 2013. Structural and thermochronometric evidence for multi-stage exhumation of southern Syros, Cycladic islands, Greece. *Tectonophysics* 595–596, 148–164.
- Spakman, W., Wortel, M.J.R., Vlaar, N.J., 1988. The Hellenic Subduction zone: a tomographic image and its geodynamic implications. *Geophys. Res. Lett.* 15, 60–63.
- Stouraiti, C., Mitropoulos, P., Tarney, J., Barreiro, B., McGrath, A.M., Baltatzis, E., 2010. Geochemistry and petrogenesis of late Miocene granitoids, Cyclades, southern Aegean: nature of source components. *Lithos* 114, 337–352.
- Teyssier, C., Whitney, D.L., 2002. Gneiss domes and orogeny. *Geology* 30 (12), 1139–1142.
- Tomaschek, F., Kennedy, A.K., Villa, I.M., Lagos, M., Ballhaus, C., 2002. Zircons from Syros, Cyclades, Greece – recrystallization and mobilization of zircon during high-pressure metamorphism. *J. Petrol.* 44, 1977–2002. <https://doi.org/10.1093/petrology/egg067>.
- Trotet, F., Jolivet, L., Vidal, O., 2001. Tectono-metamorphic evolution of Syros and Sifnos islands (Cyclades, Greece). *Tectonophysics* 338, 179–206.
- Urai, J.L., Schuiling, R.D., Jansen, J.B.H., 1990. Alpine deformation on Naxos (Greece). *Geol. Soc. London, Special Publication* 54, 509–522.
- Vandenberg, L.C., Lister, G.S., 1996. Structural analysis of basement tectonics from the Aegean metamorphic core complex of Ios, Cyclades, Greece. *J. Struct. Geol.* 18, 1437–1454.
- Vanderhaege, O., 2004. Structural development of the Naxos migmatite dome. In: Whitney, D.L., Teyssier, C., Siddoway, C.S. (Eds.), *Gneiss Domes in Orogeny: Boulder, Colorado*, vol. 380. Geological Society America, Special Paper, pp. 211–227.
- Vanderhaege, O., Teyssier, C., 2001. Partial melting and flow of orogens. *Tectonophysics* 342, 451–472.
- Van der Maar, P.A., Jansen, J.B.H., 1983. The geology of the polymetamorphic complex of Ios, Cyclades, Greece and its significance for the Cycladic Massif. *Geol. Rundsch.* 72 (1), 283–299.
- Van Hinsbergen, D.J., Hafkenscheid, E., Spakman, W., Meulenkaamp, J.E., Wortel, R., 2005. Nappe stacking resulting from subduction of oceanic and continental lithosphere below Greece. *Geology* 33, 325–328.
- Visser, R.L.M., Meijer, P.Th., 2012. Mesozoic rotation of Iberia: Subduction in the Pyrenees. *Earth Science Reviews* 110, 93–110.
- Wernicke, B., 1981. Low-angle normal faults in the Basin and Range province: nappe tectonics in an extending orogeny. *Nature* 291, 645–648.
- Wernicke, B., Burchfiel, B.C., 1982. Modes of extensional tectonics. *J. Struct. Geol.* 4, 105–115.
- Wernicke, B., Axen, G., 1988. On the role of isostasy in the evolution of normal fault systems. *Geology* 16, 848–851.
- Whitney, D.L., Teyssier, C., Rey, P., Buck, W.R., 2013. Continental and oceanic core complexes. *Geol. Soc. Am. Bull.* 125, 273–298. <https://doi.org/10.1130/B30754.1>.
- Xypolias, P., Kokkalas, S., 2006. Heterogeneous ductile deformation along a mid-crustal extruding shear zone: an example from the External Hellenides (Greece). In: Law, R.D., Searle, M.P., Godin, L. (Eds.), *Channel Flow, Ductile Extrusion, and Exhumation in Continental Collision Zones*, vol. 268. Geological Society, London, Special Publications, pp. 497–516.
- Xypolias, P., Alsop, G.I., 2014. Regional flow perturbation folding within an exhumation channel: a case study from the Cycladic Blueschists. *J. Struct. Geol.* 62, 141–155.
- Xypolias, P., Kokkalas, S., Skourlis, K., 2003. Upward extrusion and subsequent transpression as a possible mechanism for the exhumation of HP/LT rocks in Evia Island (Aegean Sea, Greece). *J. Geodyn.* 35, 303–332. [https://doi.org/10.1016/S0264-3707\(02\)00131-X](https://doi.org/10.1016/S0264-3707(02)00131-X).
- Xypolias, P., Iliopoulos, I., Chatzaras, V., Kokkalas, S., 2012. Subduction- and exhumation-related structures in the Cycladic Blueschists: insights from south Evia Island, (Aegean region, Greece). *Tectonics* 31, TC2001. <https://doi.org/10.1029/2011TC002946>.